Injury-free priming: induction of Primary Afferent Collateral Sprouting in uninjured sensory neurons *in vivo* primes them for enhanced axon outgrowth *in vitro*.

Sara Soleman[1,2], Jeffrey C. Petruska[3,*], Lawrence D.F. Moon[1,*]

[1] The Neurorestoration Group, Wolfson Centre for Age-Related Diseases, King's College London, 16–18 Newcomen Street, London SE1 1UL, UK

[2] Present address: GlaxoSmithKline, Clinical Unit Cambridge, Addenbrookes Centre for Clinical Investigation, Addenbrookes Hospital, Cambridge, CB2 0GG

[3] Dept. Anatomical Sciences and Neurobiology, Kentucky Spinal Cord Injury Research Center, University of Louisville, Department of Neurological Surgery, Louisville, Kentucky, USA.

[*] Joint Senior Authors

Joint Corresponding authors:

Dr Lawrence Moon,
Neurorestoration Group, Wolfson Centre for Age-Related Diseases,
16 – 18 Newcomen Street, London, SE1 1UL,
United Kingdom,
Tel: +44 7929 364035
Email: lawrence.moon@kcl.ac.uk

Dr Jeffrey Petruska
Dept. Anatomical Sciences and Neurobiology,
Kentucky Spinal Cord Injury Research
Center, University of Louisville,
Department of Neurological Surgery, Louisville, Kentucky, USA.
Tel: 502-852-8057
Email: j.petruska@louisville.edu

The authors declare that no conflict of interest exists.

Graphical abstract; please use Figure 1C.

Highlights: (for separate editable file)

- Others have shown that a prior conditioning lesion enhances the regeneration of DRG axons *in vivo* and predisposes them to elongate rather than arborize after dissociation of ganglia and culturing *in vitro*.
- We now show that inducing uninjured DRG neurons to undergo Primary Afferent Collateral Sprouting (PACS) into zones of denervation in the skin *in vivo* primes them for subsequent axon elongation or arborization *in vitro*.
- Transection of thoracic cutaneous nerves (T9, T10, T12, T13) created zones of denervated skin with concomitant loss of the sensory drive of the cutaneous muscle trunci (CTM) reflex.
- Over time, neurons from the uninjured T11 DRG underwent collateral sprouting within the skin which reduced the size of the zone of denervation and restored sensory drive of the CTM reflex.
- T11 DRG were dissociated either 7 or 14 days after induction of PACS and cultured in defined media lacking neurotrophins and growth factors: these neurons elongated or arborized more than naive neurons from unoperated rats.
- Microarray analysis and qRTPCR showed that that the GDNF family ligands artemin and persephin were upregulated in denervated skin at 7 and/or 14 days after induction of PACS.
- We suggest that exposure of uninjured DRG neurons to neurotrophins and growth factors in denervated skin primes them for enhanced outgrowth after explantation.

Keywords: conditioning lesion, axon regeneration, collateral sprouting, arborizing, elongation

Abstract

Prior "conditioning" nerve lesions can prime DRG neurons for enhanced axon regeneration. We tested the hypothesis that adult DRG neurons can be similarly primed for axon elongation without axonal injury through induction of Primary Afferent Collateral Sprouting (PACS). PACS was induced in uninjured T11 DRG neurons by denervating dermatomes rostrally and caudally. In this model uninjured adult DRG neurons extend uninjured axons into denervated skin in vivo. Collateral sprouting by the spared T11 DRG neurons was confirmed by mapping the expansion of its responsive zones of skin up to 14 days. At 7 or 14 days after induction of PACS, DRG neurons were dissociated and cultured without growth factors for 18 hours. Neurons from T11 PACS DRG had longer mean neurite lengths than neurons from naïve DRG. A larger proportion of neurons from T11 PACS DRG showed an elongating or arborizing phenotype than neurons from naïve DRG. DRGs serving nerves transected to create the denervated dermatomes contained large numbers of neurons expressing Activating Transcription Factor 3 (ATF3), a marker of the injury response. In contrast, T11 DRG from both unoperated rats and PACS rats contained very few neurons expressing ATF3. Microarray analyses and qRTPCR of T11 DRG and denervated/reinnervated skin reveal regulation of receptor/ligand systems as well as additional potential regulators of growth during PACS. We suggest that extracellular cues in denervated skin modify the intrinsic growth program of uninjured DRG neurons that enhances their ability to elongate or arborize even after explantation. Collectively, these data indicate that induction of PACS does not induce an injury response, yet primes many of these uninjured neurons for in vitro axon growth.

1. Introduction

After injury, axons in the central nervous system (CNS) extend collateral branches and sprout considerably but do not elongate long distances back to their original targets (Rosenzweig et al,. 2010). In contrast, after injury to the peripheral branch of the dorsal root ganglia (DRG), many sensory axons eventually elongate axons back to their original targets although this does not occur after injury to the central branch of the DRG (Snider et al., 2002). Axons from sensory neurons or motor neurons can be primed to elongate more effectively when a conditioning stimulus is given prior to an injury (Gutmann, 1942). For example, a conditioning injury to the peripheral branch of a DRG increases the number of regenerating sprouts and enhances their elongation (McQuarrie et al., 1977; McQuarrie, 1985; Richardson and Verge, 1987; Jenq et al., 1988). Indeed, a conditioning lesion has been shown to prime the cell body of axotomized neurons by activating an intrinsic transcriptional program that switches the neuron from an arborizing state into an elongating state (Smith and Skene, 1997): for example, after explantation, dissociated neurons from DRG of unoperated rats arborize after a delay whereas deliberately pre-injured DRG neurons initiate axon growth more rapidly in an elongating mode rather than an arborizing mode (Smith and Skene, 1997).

Here, we set out to test the hypothesis that DRG neurons can be primed to undergo elongation without prior injury. We took advantage of an existing, well characterised model for studying Primary Afferent Collateral Sprouting of uninjured sensory axons (Devor et al., 1979; Diamond et al., 1976; Bisby et al., 1996; Petruska et al., 2014). Cutaneous axons from one thoracic DRG almost exclusively project to a single dermatome (Ygge, 1984). One can induce sprouting of uninjured axons from a thoracic DRG into adjacent dermatomes by tranecting neighbouring thoracic cutaneous nerves (Fig 1B, C); very few, if any, neurons in the spared DRG are injured (Devor et al., 1979; Diamond et al., 1976; Bisby et al., 1996). Over a few weeks, these uninjured neurons sprout axons into adjacent, denervated dermatomes.

Accordingly, we induced PACS *in vivo* in uninjured T11 DRG neurons. Seven or fourteen days later, uninjured T11 DRG neurons were dissociated and cultured in the absence of neurotrophic factors. We compared these uninjured T11 DRG neurons with neighboring DRG with nerve injury and with neurons from T11 DRG of unoperated rats. We examined the question of whether neurons can be primed for axonal elongation without nerve injury.

2. Methods

Surgery

All procedures were in accordance with the UK Home Office and Animals (Scientific Procedures) Act of 1986, associated guidelines and the EU Directive 2010/63/EU for animal experiments. Adult female Sprague-Dawley rats (*n*=7) were anesthetized with isoflurane. Fur was removed from the thoracolumbar region of the back and a 4 to 5 cm longitudinal incision of the skin was made approximately 1 cm to the right of the midline and clipped back. The off-midline incision was performed to avoid cutting left-side sensory axons which induces an injured state (Hill et al, 2010; Rau et al., 2016). Blunt dissection of subcutaneous fascia exposed the array of dorsal cutaneous nerves (DCNs) and lateral cutaneous nerves (LCNs). Thoracic (T) T9, T10, T12 and T13 DCNs and LCNs were identified (Fig. 1A) and carefully freed from both connective tissue and the latissimus dorsi muscle wall. These cutaneous nerves were then transected a few millimetres from the body wall and ligated with 7-0 Ethilon sutures (Fig. 1B). This procedure successfully disallows nerve regeneration to the skin in almost every instance (Diamond et al., 1992b). The T11 DCNs and LCNs were left intact, with the T11 sensory field "isolated" within a relatively vast area of denervated skin (Fig. 1B). The DCNs and LCNs were both transected in this experiment in order to provide a greater area of neighbouring denervation around the spared T11 dermatome than if only the DCNs were transected. The skin incision was then closed. Before animals were allowed to recover from anaesthesia, mechanonociceptive fields were mapped as described below. Rats were terminally anesthetized at day 7 (n=4) or day 14 (n=3) because it is known that PACS occurs during this time frame. Analgesic (buprenorphine, 0.01 mg/kg subcutaneously) was given for 3 days after surgery.

At the end of the survival period (7 or 14 days post-surgery), animals were deeply anesthetized and the DRGs were retrieved either unfixed or fixed (see below). To ensure isolation of the correct DRGs, the spared and transected cutaneous nerves were traced back through the *latissimus dorsi* muscle to the ganglion cell body via microdissection.

This surgery provided both uninjured neurons undergoing PACS (T11 DRG) and transected neurons (T9, 10, 12, 13 DRG). We retrieved the corresponding contralateral DRGs to use as a comparison group. However, we must note that these contralateral DRGs likely contain a small number of neurons that have been injured by the incision (Hill et al 2010; Rau et al 2016) and some innervating the peri-incisional skin that may have been induced into the PACS-state by the local inflammation. "Naive" T11 DRG were also retrieved from unoperated rats (n=3).

DRG neurons explanted from naive (unoperated) rats will be referred to as "naive DRG" and "naive neurons", although clearly the explant procedure induces an injury. T11 "PACS DRG" will be used to refer to uninjured, T11 DRG which underwent PACS prior to explantation. "Transected DRG" will be used to refer to thoracic DRG whose nerves had been transected.

Behavioural mapping of nociceptive fields

A simple behavioural test involving the *cutaneous trunci* muscle (CTM) reflex system was used to monitor progress of collateral sprouting, synapse formation and functional recovery (Diamond et al., 1987; Doucette and Diamond, 1987; Diamond et al., 1992b). Mechanonociceptive fields were "pinch mapped" under light isoflurane anaesthesia, a level

that enabled brisk but localised reflex responses to pinching of the skin or foot. Fine-toothed forceps were used to pinch the skin which evokes a reflex contraction of the underlying *cutaneous trunci* muscle (CTM), causing a visible contraction of the skin (Fig. 2A, B) (Therieault and Diamond 1998; Petruska et al., 2014; Harrison et al., 2015; Rau et al 2016). The borders between sensitive and insensitive areas of the skin were determined by the respective presence or absence of the CTM response to successive mechanonociceptive stimulus at approximately 2 to 3 mm intervals. The skin was marked using a permanent marker between unresponsive and responsive test sites, to assess the field expansion over time (Fig. 1C and Fig. 2C, D). It should be noted that nociceptive dermatomes overlap such that denervation of at least two adjacent dermatomes was required to generate a "nociceptor-denervated" area of skin. When a cutaneous nerve field was expanded by collateral sprouting, so did the area of the evoked CTM reflex (Pertens et al., 1999).

Immunolabelling for ATF3 to assess injury status of DRG neurons

An additional set of adult female Sprague-Dawley rats (260-310 g) was anesthetized with pentobarbital (65 mg/kg, i.p.). Sprouting of T11 DRG neurons was induced with surgical isolation of cutaneous sensory fields by unilateral transection of T9, T10, T12, and T13 of dorsal and lateral cutaneous nerves (Figure 1). In the operated rats, denervation of the dermatomes was confirmed by lack of CTM reflex in response to pinch. We used CTM reflex testing to confirm success of PACS. In addition, one rat received transection of the sciatic nerve at mid-thigh level and was perfused 7 days later. Analgesic (buprenorphine, 0.01 mg/kg subcutaneously) was given for 3 days after surgery. Seven or Fourteen days after surgery, rats were deeply anesthetized with pentobarbital (65 mg/kg, i.p.) and perfused transcardially with saline followed by 4% paraformaldehyde in 0.1 M phosphate buffer. Spinal cord and DRGs were removed and post-fixed in 4% paraformaldehyde overnight. Tissue was transferred to a solution of 20% sucrose (Sigma, Poole, UK) for at least 24 hours at 4°C.

DRG sections were cut at a thickness of 10 µm on a cryostat. Sections of DRG were mounted onto Superfrost Plus slides (BDH, Poole, UK). Sections were air dried and incubated in 2% normal goat serum in 0.1 M Tris-buffered saline (TBS) containing 0.2% Triton X-100 for 60 min. Sections were then incubated in rabbit polyclonal anti-ATF3 antibody (1:500, overnight; Santa Cruz, CA) in 0.1 M Tris-buffered saline (TBS) containing 0.2% Triton X-100. Sections were washed in TBS containing 0.2% Triton X-100 three times and incubated in Alexa 488-conjugated goat anti-rabbit secondary antibody (1:500, 4 hours; Invitrogen) containing bisbenzimide (1 µg/ml). They were washed in TBS containing 0.2% Triton X-100 three times and washed in distilled water. Sections were mounted onto coverslip in Vectashield medium (Vector). Control sections were treated in the same manner, but with 10% normal goat serum replacing the primary antibody.

Primary DRG cultures

DRG from T9 to T13 on both the ipsilateral and contralateral side to surgery were collected and placed in individual wells of a 24 well plate containing Hams F-12 media (Life Technologies, Gaithersburg, MD). Ganglia were cleared of connective tissue, and individually incubated in 0.125% collagenase and 50 µg/ml DNase (Sigma) for 2.5 hr at 37°C in 5% CO_2, to chemically dissociate and prevent cell clumping during tissue disaggregation. Ganglia were then mechanically dissociated individually by gentle trituration in 1 ml of F-12

media then centrifuged through a 15% BSA cushion at 700 rpm (77 x g) for 7 min. Dissociated neurons were re-suspended in 100 µl of modified Bottenstein and Satos medium (BS): Neurobasal media (Invitrogen) supplemented with 100 units/ml BSA (30%; Sigma), 100 units/ml N2-supplement (Invitrogen), 100 units/ml penicillin and 100µg/ml streptomycin (Invitrogen). This defined medium lacks neurotrophins and growth factors including NGF, BDNF and GDNF. Cells were then plated onto Lab-Tek (Nunc, Fisher Scientific, Loughborough, UK) chamber slides coated with poly-L-lysine (2 mg/ml; Sigma). As the dissociation of individual ganglions generally retrieved between 800-1000 cells, the suspension was divided into only two chambers to provide low-density cultures. Cultures were incubated for 18 hr at 37°C in a humidified atmosphere containing 5% CO_2.

Immunocytochemistry

Cells were fixed with 4% PFA for 20 min at room temperature, then permeabilized with methanol (100%) for 3 min and washed 3 times in PBS. To assess neurite outgrowth, all cells were incubated in the following: mouse anti-βIII tubulin (1:1000; 2 hr; Promega) and goat anti-mouse Alexa 546 (1:1000; 45 min; Molecular Probes, Invitrogen). Lab-Tek chambers were removed and slides were coverslipped with Vectashield mounting medium with DAPI (Vector Labs).

Quantitative analysis of neurite outgrowth

All images were captured using a Carl Zeiss AxioImager Z1 microscope and analysed by an investigator blinded to different groups. Analysis was organised into the following groups: 1) Spared T11 DRG, 2) Transected DRGs (all values for individual transected DRGs were pooled for analysis), 3) Contralateral spared T11 DRG, and 4) Contralateral-to-transected DRGs (T9, T10, T12, T13 were pooled for analysis).

Analysis of neurite outgrowth: The number of sprouting neurons, visualised by βIII tubulin immunoreactivity, were quantified using two parameters: all sprouting neurons with neurites extending longer than 10 µm or greater than 50 µm. The percentage of sprouting neurons was calculated as follows: (number of sprouting neurons/total number of neurons) x 100. The total number of neurons per well ranged from 150 – 500 cells.

Sholl analysis: Neurons with projections greater than 50 µm were analysed using Sholl analysis to determine the total neurite length and number of branches at each shell distance. Grayscale 8-bit images were obtained and semi-automatically traced with NIH Image J using the Sholl Analysis plug-in. Analysis parameters for the concentric circles included: starting radius = 50 µm from the centre of the neuron, radius step intervals = 50 µm and ending radius = 900 µm.

Neurons with a mean of <2 branches per 100 µm neurite were categorised as elongating, whereas those with mean >2 branches per 100 µm neurite were categorised as arborizing.

Analysis of cell size distributions: Cell size distributions were also determined using the AxioVision LE V4.7.2 (Carl Zeiss) contour tracing software. Cell diameter (µm) was measured in all sprouting neurons extending processes greater than 50 µm and tabulated for each group.

Real time qRTPCR

In a previous study, to identify genes that were regulated in uninjured T11 DRG neurons during PACS, we performed microarray analysis upon RNA taken from T11 DRG from naïve rats (n=5) and from T11 DRG taken 7 days (n=7) or 14 days (n=7) after induction of PACS (Harrison et al., 2015; Harrison et al., 2016). Microarray analysis was also performed using RNA from those same rats from intact skin (n=6) or 7-day denervated skin (n=5) and 14-day denervated skin (n=5) (Flight et al., 2014). Those datasets may be found at the Gene Expression Omnibus (GEO) with accession numbers GSE72551 (DRG) and GSE54356 (skin).

Here, we used qRTPCR to confirm some of the gene changes identified during microarray analysis. Some results have been presented previously (Harrison et al., 2015). We used aRNA left over from the first round of amplification prior to microarray analysis. 200 ng aRNA, 2 µl of Random Primers (250 ng/µl, Invitrogen) and Nuclease-free water (Qiagen) were mixed to total volume 12 µl, and then heated at 70˚C for 3 minutes. Then first strand cDNA synthesis was carried out using 1 µl M-MLV Reverse Transcriptase (Ambion Research), 1 µl RNase inhibitor, 2 µl reaction buffer and 4 µl dNTP mix to 20 µl total volume. They were incubated for 1 hour at 42˚C, and to inactivate reverse transcriptase heated for 10 minutes at 92˚C. To construct standard curve for genes of interest total RNA was extracted from homogenized head of 15/16 days rat embryo (Fischer 344) by TRIzol reagent (Invitrogen). 5 µg total RNA was treated with DNase (Qiagen) and purified (RNeasy Kit, Qiagen). cDNA was produced by using Random Primers (250 ng/µl, Invitrogen) and SuperScript II reverse transcriptase (Invitrogen).

The primer sequences are taken from Primer Bank or were designed based on the probe set target sequence provided by Affymetrix using Primer3 software (www.genome.wi.mit.edu) (Table 1). Quantitative analysis was carried out by real-time PCR (Rotor-Gene 3000, Corbett Life Science, Sydney, Australia). Each reaction contained cDNA, 0.5 µl of each primer (25 ng/µl), 12.5 µl of 2X SYBR Green PCR Master Mix (AmpliTaq Gold DNA polymerase, reaction buffer, dNTP mix, 2X SYBR Green 1 dye; Applied Biosystems) in 25-µl reaction. Reactions were performed in triplicate for standard curve. GAPDH was selected as control gene because microarray analysis indicated it was invariant in DRG during PACS. Standard curves of genes of interest and endogenous control GAPDH gene were constructed with eight 3-fold dilutions of cDNA from E15/E16 rat head. The amplification program consisted of 1 cycle at 95ºC for 10 min followed by 40 cycles of 95ºC denaturation for 15 s, 60ºC annealing and extension for 60 s. For melting curve analysis the samples were heated from 60ºC to 95ºC. Single melting curve peaks indicated that a single product was amplified. Amplified products were also run on a 1% agarose gel to show the specificity of the amplicon. After raw data was collected, the data was normalized to account for initial differences in background fluorescence. The fold change was expressed relative to GAPDH value.

Statistical Analysis

Analysis was performed using SPSS (V17.0). The percentage of neurons that sprouted, the percentage of sprouting neurons that were elongating or arborizing, and the percentage of sprouting neurons that were large/small diameter neurons were analysed using either the Mann Whitney (independent samples from different rats *e.g.*, naive vs. spared T11 neurons)

or Wilcoxon (related samples) tests. Data from the Sholl analysis for branch number and neurite length was analysed using two way repeated measures analysis of variance (RM ANOVA) with factors of group and time. Where interactions were significant, pairwise group comparisons were conducted using Fisher's Least Significant Difference (LSD) *post hoc* tests and exact p-values are reported. To avoid visual and textual clutter, we do not report differences relative to contralateral T11 neurons and to contralateral-to-transected neurons. qRTPCR data were analysed using ANOVA followed by LSD *post hoc* tests. In all cases, *post hoc* tests were reported only when the ANOVA was significant ($p<0.05$). Data is presented as means ± SEM and asterisks indicate significance as follows: *$p\leq0.05$; **$p\leq0.01$; ***$p\leq0.001$.

3. Results

Spared dermatome surgery induced expansion of mechanonociceptive "pinch" fields by uninjured neurons

Mechanonociceptive fields were "pinch mapped" under light isoflurane anaesthesia using fine-toothed forceps. In unoperated rats, this evokes a visible reflex contraction of the skin (Fig. 2A, B) above the *cutaneous trunci* muscle (CTM). As expected, immediately after surgery, the CTM reflex response was present in the skin innervated by the spared T11 cutaneous nerves (zone shown in blue; Fig. 2C) and absent in adjacent zones denervated by transection of cutaneous nerves (zone shown in red; Fig. 2C). At 14 days after induction of PACS, behavioural mapping of borders between responsive and unresponsive areas revealed receptive field expansion (Fig 2D; white arrows) relative to previous borders (black arrows). Thus, this revealed expansion of the "isolated" mechanonociceptive sensory field (denoted by blue line) and a decrease in the area of denervated skin (denoted by red lines), consistent with previous studies showing that this expansion and restoration of function is due to the Primary Afferent Collateral Sprouting by intact fibers from the spared T11 DRG (Diamond et al., 1992b; Doucette and Diamond, 1987; Nixon et al., 1984).

A subgroup of rats received the same surgery but was perfusion-fixed and DRG sections were immunolabelled using an antibody against ATF3. As expected, T11 DRGs from naïve rats contained few or no neurons that were positive for ATF3 (Figure 3A) whereas DRGs containing neurons that were injured by nerve transection contained many neurons that were positive for ATF3 (Figure 3B) (Hill et al., 2010). Few or no neurons from T11 DRG taken 7 or 14 days after induction of PACS were positive for ATF3 (Fig 3C and 3D). Importantly, we had used CTM reflex testing to verify expansion of receptive fields in these rats to prove that they had undergone PACS *in vivo* prior to removal of tissues. These data show that T11 DRG neurons from rats undergoing PACS do not express ATF3: this confirms that our surgical procedure does not injure the T11 DRG neurons before they are explanted for culturing (see below). This is consistent with our microarray data which did not show any evidence of regulation of ATF3 mRNA in DRG at 7 or 14 days after induction of PACS (ANOVA $p>0.05$) (Harrison et al., 2015).

Induction of PACS primes neurons for enhanced neurite outgrowth

To determine a suitable time-point to assess neurite outgrowth, DRG neurons from naive rats were isolated and cultured in defined media for 18 hours (Fig 4A, B) or 24 hours (Fig 4C, D). In line with previous studies of dissociated mature primary DRG neurons (Smith and Skene, 1997; Cafferty et al., 2004), the majority of naive neurons failed to extend many neurites after 18 hr *in vitro* and those that did had short processes (Fig 4B). In comparison, after 24 hr *in vitro* many naive neurons had sprouted with some extending long neurites (Fig 4D). Accordingly, we assessed outgrowth 18 h following induction of PACS. Successful PACS *in vivo* was confirmed by "pinch mapping" before DRG were harvested for *in vitro* testing.

Neurons from naive DRG extended short or no neurites whereas neurons from PACS or transected DRG showed increased elongation (Figure 5) and/or arborization (Figure 6). Seven days after surgery, some neurons from PACS DRG had neurites longer than 50 µm (Fig 5A); neurite lengths were greater in neurons from transected DRG, which extended up to 700 µm (Figure 5B). Neurite lengths of neurons from contralateral T11 DRG (Figure 5C) and

contralateral-to-transected DRG (Figure 5D) were short. Fourteen days after surgery, some neurons from transected DRG and PACS DRG had long, sparsely branched neurites (Figure 5E-G). Some transected neurons extended neurites over 900 µm (Figure 5G). Some neurons from PACS DRG extended fairly long processes (Figure 5E) including in excess of 900 µm (Figure 5F).

Other neurons from transected DRG and PACS DRG had highly branched neurites with lengths extending up to 400 µm at 7 days (Figures 6A-B) and up to 550 µm at 14 days (Figures 6E-F). In contrast, neurons from control DRG (contralateral-to-transection) had many branches and short neurite lengths at 7 days (Figures 6C-D) and 14 days (Figures 6G-H).

The percentage of neurons initiating neurite outgrowth greater than 10 µm was first quantified (Figure 7A-B). Few naive neurons extended neurites greater than 10 µm (0.98 ± 0.1%). In contrast, relative to naïve neurons a greater percentage of both PACS neurons and transected neurons extended processes greater than 10 µm (naive vs. 7 days, p=0.007; naive vs. 14 days, p=0.01; Fig 7B). There was a larger percentage of neurons with neurites longer than 50 µm in neurons from transected DRG compared to naive neurons (naive vs. 7 days, p=0.007, naive vs. 14 days, p=0.01; Fig 7D) and in PACS neurons compared to naïve neurons (7 days, p=0.02; 14 days, p=0.03). Overall, PACS neurons had longer neurites than naive neurons (7 days, p=0.03; 14 days, p=0.04; Figure 7E) and transected neurons had longer neurites than naive neurons (naive vs. 7 days, p=0.02; naive vs. 14 days, p=0.02).

The process of PACS *in vivo* might involve both axonal elongation and arborization to re-innervate large volumes of skin. Using Sholl analysis (Fig. 7A, C), neurons with a mean of <2 branches per 100 µm neurite were categorised as elongating, whereas those with mean >2 branches per 100 µm neurite were categorised as arborizing. Examples of DRG neurons categorised as "elongating" or "arborizing" can be seen in Figures 5 and 6, respectively. These two groups were analysed separately.

A greater proportion percentage of neurons showed arborization after induction of PACS or transection than in naive DRG.

A larger percentage of neurons from PACS DRG were categorised as elongating than those from naïve DRG at 7 days (p=0.03; Fig 8A) and at 14 days (p=0.04). A larger percentage of neurons from transected DRG were categorised as elongating relative to those from naïve DRG at 7 (p=0.05) and 14 days (p=0.02) The percentage of neurons categorised as elongating increased from 7 to 14 days after surgery in transected neurons (p=0.001) and showed a strong trend in PACS neurons (p=0.07).

A larger percentage of neurons from PACS DRG were categorized as arborizing than those from naive DRG at 14 days (p=0.04; Fig. 8B) but not at 7 days (p=0.29). A larger percentage of neurons from transected DRG were categorized as arborizing than those from naive DRG at 14 days (p=0.04) and there was a trend at 7 days (p=0.09).

The results of the Scholl analysis are presented in Figure 9.

Small diameter neurons account for the majority of sprouting neurons in vitro

A histogram was plotted showing the distribution of soma sizes for all sprouting neurons from the uninjured T11 DRG (Fig 11A). Separate histograms were then plotted for elongating

(Fig 11C) and arborizing neurons (Fig 11E). Next, we categorised each neuron as having a small diameter (<35 µm) or a large diameter (>35 µm) *in vitro*. Of the neurons that sprouted, a greater proportion had a small diameter than a large diameter at seven and fourteen days after induction of PACS (7 days, p=0.01; 14 days, p=0.05; Fig 11B). There was no difference over time in the proportion of sprouting neurons with a small diameter (7 vs. 14 days, p=0.2).

Elongation: A greater proportion of elongating neurons had a small diameter than a large diameter (7 days, p=0.02; 14 days, p=0.05; Fig 11D). There was no difference over time in the proportion of sprouting neurons with a small diameter (7 vs. 14 days, p=0.4).

Arborisation: A greater proportion of arborising neurons had a small diameter than a large diameter (7 days, p=0.01; 14 days, p=0.05; Fig 11F). There was no difference over time in the proportion of sprouting neurons with a small diameter (7 vs. 14 days, p=0.2).

Collectively, this data suggests that the population responsible for the sprouting observed *in vitro* are small diameter neurons.

The majority of sprouting neurons are CGRP negative

Previous studies have reported that Aδ (Nixon et al., 1984) and C fibers from uninjured DRG neurons undergo Primary Afferent Collateral Sprouting *in vivo* (Doucette and Diamond, 1987). Others have shown that conventional conditioning lesions induce a growth state in some but not all types of DRG neurons (Kalous and Keast, 2010). We therefore sought to identify which subtypes of T11 DRG neurons undergo enhanced neurite outgrowth *in vitro* following induction of PACS *in vivo*. We identified sprouting neurons by immunolabeling for beta III tubulin and we co-immunolabelled for the peptide CGRP (Figure 12).

Although a small percentage of T11 DRG neurons were CGRP positive, a greater percentage were CGRP negative at both time-points after induction of PACS (Fig 11A-C) (7 days, p=0.02; 14 days p=0.05). A greater percentage of neurons from transected DRG were CGRP negative than CGRP positive at 7 days (p=0.001) and at 14 days (p=0.004) (Figure 11A).

T11 neurons undergoing PACS express mRNA for receptors whose ligands are regulated in denervated skin

We have previously performed microarray analysis using RNA from T11 DRG or denervated skin taken from naïve rats or from rats 7 days or 14 days after induction of PACS *in vivo* (Flight et al., 2014; Harrison et al., 2015; Harrison et al., 2016). Tables 2 and 3 show the genes in DRG and skin (respectively) that were evaluated by real time qRTPCR; results obtained using dChip for microarray analysis are also presented for comparison. As expected, microarray analysis showed that markers of neuronal injury were not regulated in T11 DRG at 7 or 14 days (*e.g.*, activating transcription factor 3; colony stimulating factor 1; p-values>0.05).

We were interested to determine whether there were changes in expression level in DRG for receptors for ligands whose levels were altered in denervated skin, particularly those known to be expressed by small diameter neurons that sprout in response to induction of PACS *in vivo* and *in vitro* (including NGF and GDNF family receptors and ligands). Others have shown that NGF mRNA is increased in skin, for example (Mearow et al 1993). Surprisingly, our microarray analysis did not detect upregulation of Nerve Growth Factor mRNA in skin

(NGF beta probe set 1371259_at; NGF gamma probe set 1367961_at); however, qRTPCR using two different primer pairs (Table 1) confirmed that NGF beta mRNA was upregulated (~3-fold) in skin at 7 days and 14 days (Table 3). Although microarray analysis did not detect changes in TrkA in DRG (Table 2), qRTPCR identified trends towards decreases at day 7 and 14 (Table 3). qRTPCR showed that p75NTR was also upregulated in skin at 7d but not 14 after induction of PACS (Table 3) but not in DRG at 7 or 14 days (Table 2). These changes in p75 receptor in skin and TrkA receptor in DRG might counteract the effects of increases in NGF in skin upon sprouting.

Small diameter DRG neurons are also known to express receptors for GDNF family receptor alpha (GFRα) 1, 2, 3 and 4 and c-ret (Bennett et al., 1998; Bennett et al 2000). Interestingly, the GDNF family ligand, Persephin, was shown by microarray analysis and qRTPCR to be regulated in skin at 14 days after induction of PACS (Table 3). qRTPCR showed that Artemin, another GDNF family ligand, was upregulated in skin at 7d and 14 days after induction of PACS (Table 3) [*n.b.*, Artemin was not represented by a probe set on the microarray chips]. There was no evidence that GDNF or neurturin was regulated in skin by either microarray analysis or qRTPCR (Table 3). Regarding receptors, qRTPCR found evidence for downregulation in DRG of GFRα4 at 7 and 14 days (Table 2) although this was not detected by microarray analysis. Microarray analysis indicated slight upregulation of GFRα2 in DRG at 14 days but this was no validated by qRTPCR (Table 2). There was no evidence for regulation of GFRα1 or GFRα3 or Ret isoform b by either method in DRG but there was evidence that Ret isoform a was regulated in skin at 14 days by both microarray and qRTPCR (Table 3).

Large diameter DRG neurons serving low-threshold mechanoreception functions in the skin express the TrkC receptor for neurotrophin-3 (NT-3; McMahon et al 1994; Krimm et al., 2000) and the available evidence indicates that these axons do not sprout during PACS (Jackson and Diamond, 1983, 1984; Horch 1981). Consistent with this, microarray analysis showed evidence for slight downregulation of NT-3 in skin (-1.2 fold) at both 7 days and 14 days (Table 3) although qRTPCR did not confirm any regulation; above all, there was no evidence for upregulation of NT-3 in skin and this may account for the failure of sprouting of TrkC expressing DRG neurons during PACS. Microarray analysis also showed evidence for downregulation of TrkC in DRG by 1.2 fold at both 7 days and 14 days (Table 2) although qRTPCR did not confirm this.

Finally, qRTPCR validated other changes in gene expression in T11 DRG at 7 and 14 days after induction of PACS including BDNF, Frzb, Grhl3, Spp1 (osteopontin) and Enpp3, Cacna2d1 and Gadd45a (Table 2). Future work may determine whether these genes are involved in priming of DRG neurons for outgrowth once dissociated and maintained in defined media lacking neurotrophins and growth factors *in vitro*.

4. Discussion

Adult mammalian sensory neurons are capable either of axonal regeneration of cut axons or of collateral sprouting of non-injured axons induced by various stimuli including loss of neighboring innervation (Mahar and Cavalli, 2018; Lorenzana et al., 2015). Prior injury ("conditioning") is known to induce an enhanced axonal outgrowth when sensory neurons are subsequently grown *in vitro* (Smith & Skene, 1990). It was not known if the changes induced by collateral sprouting *in vivo* may prime uninjured neurons for enhanced growth *in vitro*.

As expected, the transection of multiple thoracic cutaneous nerves either side of the uninjured T11 nerves produced a CTM-responsive region isolated by areas that initially did not exhibit CTM reflex responses. The responsive region expanded over 7 to 14 days into previously unresponsive areas (Jackson and Diamond, 1981; Nixon et al., 1984; Diamond et al., 1987; Doucette and Diamond, 1987; Diamond et al., 1992b; Pertens et al., 1999): this confirms that uninjured axons sprouted and restored functionally useful connections (Isaacson and Crutcher, 1998; Jackson and Diamond, 1981; Doucette and Diamond, 1987; Jackson and Diamond, 1984).

Next, we investigated whether that the neurons undergoing PACS were injured during surgery by immunolabeling for an injury-related protein (ATF3) (Tsujino et al 2000). As expected, immunolabeling confirmed that T11 DRG from unoperated rats and T11 DRG at day 7 or 14 after induction of PACS contained very few ATF3 positive neurons whereas DRG with transected nerves contained large numbers of ATF3 positive neurons. This confirmed that neurons undergoing PACS were not injured.

Induction of PACS primed DRG neurons for axonal elongation or arborization in vitro

We dissociated DRG neurons seven or fourteen days after induction of PACS and grew them for 18h in defined media lacking growth factors or neurotrophins. A larger proportion of PACS neurons extended neurites than naive neurons. Those PACS neurons that sprouted a process were categorised as having elongated or arborized; the elongated form appeared more prevalent at 7 and 14 days after induction of PACS. Others had previously shown that a conditioning lesion causes injured neurons to initiate extension of neurites more rapidly in vitro and that neurites tend to elongate rather than arborize (Kalous and Keast, 2010; Cafferty et al., 2004; Cafferty et al., 2001; Smith and Skene, 1997). Our experiments extend these results and show that an accelerated growth process can also be initiated without injury by induction of collateral sprouting *in vivo*.

Although the absolute proportion of PACS neurons that sprouted may appear small, it is much larger when considered relative to the subpopulation that would be affected in this surgical model. This model does not denervate the entire dermatome of the neighboring segments: only the dorsal and lateral cutaneous nerves (DCn; LCn) were transected, leaving the ventral cutaneous nerves (VCn) intact. Thus, only those neurons with axons innervating that portion of the T11 dermatome served by the DCn and LCn (but not VCn) would be subjected to a PACS-inducing environment. This is in the range of only 40% of the DRG neurons in the rat T11 DRG (Hill et al., 2010). The remainder of the T11 DRG serves targets not denervated in the PACS model, including viscera and muscles (which therefore one

would expect not to sprout). Approximately 5% of the total number of T11 PACS DRG neurons displayed axonal outgrowth. This 5% of the total population is 12.5% of the total sub-population exposed to a PACS-inducing environment, as defined by neurons with axons in the DCn or LCn. Of those DRG neurons projecting axons through the DCn or LCn, some subtypes are known to not undergo PACS (see below), and others may project to a central portion of the T11 dermatome which is likely to be less-influenced by denervation of the neighboring dermatomes. In summary, our results show that a significant proportion of PACS-primable uninjured neurons underwent enhanced growth *in vitro*.

Phenotype of neurons that sprouted in vitro after induction of PACS

Conditioning lesions induce a growth state in some but not all types of injured DRG neurons (Kalous and Keast, 2010). What is the phenotype of uninjured neurons that are primed by PACS? Previous studies have reported that Aδ (Nixon et al., 1984) and C fibers from uninjured DRG neurons undergo Primary Afferent Collateral Sprouting *in vivo*, in contrast to large-diameter A-fiber neurons (Doucette and Diamond, 1987; Horch 1981). We found that the majority of neurons sprouting after PACS were small-diameter neurons which may include unmyelinated C fibers and also myelinated Aδ fibers. Immunolabeling revealed that some neurons undergoing sprouting were CGRP-positive but that the majority were CGRP-negative. Considering these each in turn:

<u>CGRP-positive neurons</u>: These TrkA-positive afferents are capable of robust PACS and that this collateral sprouting is a robust, rapid growth response to an acute denervation that is dependent on NGF (Diamond et al., 1992b; Diamond et al., 1987; Doucette and Diamond, 1987; Mearow et al., 1993; Pertens et al., 1999).

<u>CGRP-negative neurons:</u> Why are CGRP-negative neurons primed to sprout *in vitro* after induction of PACS *in vivo*? **1)** One possibility is that CGRP-positive neurons secrete a factor within the DRG that primes its CGRP-negative neighbours: candidates might include BDNF (see below). **2)** Another possibility is that CGRP-negative neurons undergo PACS *in vivo* which then primes them for growth *in vitro*. However, if CGRP-negative neurons do undergo PACS *in vivo* then they have been overlooked to date: **a)** silver staining indicated that collateral sprouting is halted by anti-NGF treatments that is designed to block growth by the TrkA-positive, CGRP-positive neurons (Diamond et al., 1992b). However, these silver stains would not have detected any CGRP-negative, unmyelinated axons because the method preferentially labels neurofilament proteins which are largely absent in unmyelinated axons but which are present in Aδ axons (many of which are trkA+/CGRP+) (Gambetti et al., 1981; Phillips et al., 1983; Dahl et al., 1981). **b)** Moreover, if CGRP-negative neurons do undergo PACS *in vivo* then they may not be capable of forming synapses that drive the CTM reflex: it is the TrkA-positive (CGRP-positive) neurons which drive the CTM reflex in uninjured rats (Petruska et al., 2014). Evidence for this is that the CTM reflex is absent in rats where TrkA-positive neurons have been ablated using a neurotoxin which spared other small neurons (binding IB4 or being positive for somatostatin or P2X3). **3)** The third possibility is that CGRP-negative neurons do not undergo PACS *in vivo* but exposure to the denervated skin primes them for subsequent growth *in vitro*.

What, then, is the phenotype of the CGRP-negative neurons that sprout *in vitro*? The CGRP-negative population is often characterized by their binding of the lectin IB4, but this

binding is rapidly lost upon dissociation and culturing unless growth factors are added (Averill et al., 2004), precluding our use of IB4-binding (given our choice of media). We propose that these CGRP-negative small-diameter neurons are almost certainly cutaneous (as most visceral and muscular small-diameter neurons express CGRP (e.g., Bennett et al., 1996), and are therefore likely in the sub-population exposed to a PACS-inducing environment by the spared dermatome surgery. It is possible that some of the small-diameter, CGRP-negative neurons that sprout *in vitro* express GDNF receptors (Bennett et al., 1998; Bennett et al., 2000) because, as described next, ligands for these receptors are increased in the denervated skin. Future experiments could address this possibility directly.

Induction of PACS alters gene expression in DRG and in denervated skin

We previously used microarray analysis to identify genes that are differentially regulated in uninjured T11 DRG neurons undergoing PACS (Harrison et al., 2015; Harrison et al., 2016) and in the corresponding denervated skin (Flight et al,. 2014). In comparison to naive neurons, significant differences in gene expression were found in hundreds of genes at 7 and 14 days after surgery in both PACS DRGs and denervated skin. More genes and biological processes achieved statistical significance at 14 days after surgery than 7 days after surgery. Might exposure of uninjured DRG neurons to secreted factors in the denervated skin prime their intrinsic transcriptional program for axon growth that persists after being explanted and grown in media lacking neurotrophins and growth factors?

Genes that were upregulated in the skin included NGF. This supports evidence found by other researchers previously (Mearow et al 1993) and it may explain the sprouting of TrkA-positive axons. Other genes that were upregulated in skin included the GDNF family ligands Persephin and Artemin. This is interesting because some small-diameter DRG neurons are known to express receptors for these and other GDNF family ligands including GDNF receptor alpha (GFRα) 1, 2, 3 and 4 and c-ret (Bennett et al., 1999; Bennett et al., 2000). It is possible therefore that these GFRα-positive (TrkA-negative) neurons sprout during PACS (although see comments above). Future work may show whether neurons expressing GFRa receptors undergo PACS (by responding to GDNF family ligands) and become primed for enhanced outgrowth *in vitro*.

The role of target-derived factors in the priming effect we have described is not clear. It is possible that the PACS environment triggers an intrinsic change in the DRG neurons which is carried into the explanted assay system independent of the presence of the factors. Alternatively, the enhanced growth state may be due to the expression of a gene program enabling receptivity to extrinsic factors, and the presence of the extrinsic factors is then required. In this case, the priming we observe may be "residual", in that it is the offset of the actual growth pattern/rate that might be observed in vivo.

It is therefore interesting that other genes were found to be regulated in the DRG during PACS, including BDNF (Harrison et al., 2015) which is already known to be a neuronally-expressed growth-associated gene. The role for this BDNF up-regulation and the cells that synthesize BDNF during PACS remains unknown. Interestingly, the up-regulation of BDNF in neurons observed following PACS may be in response to the significant increase of NGF in the skin (Mearow et al., 1993; see also Apfel et al., 1996; Michael et al., 1997). Increased synthesis of BDNF by DRG neurons can certainly enhance sensory axon outgrowth *in vitro* (Blits et al., 2003).

5. Conclusions

The findings presented here provide evidence that induction of PACS *in vivo* activates a growth response in uninjured neurons which enhances neurite outgrowth after subsequent dissociation. Our results demonstrate that uninjured neurons that underwent PACS show enhanced neurite outgrowth involving axonal elongation and/or arborization. Analysis of genes expressed by uninjured neurons undergoing PACS may help identify factors that enhance axon elongation or arborization. Conditional deletion of NGF or GDNF-family ligands in skin (or their receptors in DRG) could be performed after induction of PACS. Alternatively, these ligands might be supplemented to facilitate axonal growth and functional recovery after damage to skin or the CNS, or inhibited in cases where PACS-like process are maladaptive.

Acknowledgments

Yunhee Lee and Rebecca Hall performed real time qRTPCR. This work was funded by a grant from the MRC (G0600998) to Dr. Moon, and from the National Institutes of Health (NS094741) to Dr. Petruska. The funding agencies had no involvement in the planning or execution of the study. All three authors designed the research, JP and SS did surgeries, SS analysed data and all three authors contributed to writing the paper.

Reference List

Abbadie C, Basbaum AI (1998) The contribution of capsaicin-sensitive afferents to the dorsal root ganglion sprouting of sympathetic axons after peripheral nerve injury in the rat. Neurosci Lett 253:143-146.

Apfel SC, Wright DE, Wiideman AM, Dormia C, Snider WD, Kessler JA (1996) Nerve growth factor regulates the expression of brain-derived neurotrophic factor mRNA in the peripheral nervous system. Mol Cell Neurosci 7:134-142.

Aszmann OC, Muse V, Dellon AL (1996) Evidence in support of collateral sprouting after sensory nerve resection. Ann Plast Surg 37:520-525.

Averill S, Michael GJ, Shortland PJ, Leavesley RC, King VR, Bradbury EJ, McMahon SB, Priestley JV (2004) NGF and GDNF ameliorate the increase in ATF3 expression which occurs in dorsal root ganglion cells in response to peripheral nerve injury. Eur J Neurosci 19:1437-45.

Bennett DL, Dmietrieva N, Priestley JV, Clary D, McMahon SB (1996) trkA, CGRP and IB4 expression in retrogradely labelled cutaneous and visceral primary sensory neurones in the rat. Neurosci Lett 206:33-36.

Bennett DL, Michael GJ, Ramachandran N, Munson JB, Averill S, Yan Q, McMahon SB, Priestley JV (1998) A distinct subgroup of small DRG cells express GDNF receptor components and GDNF is protective for these neurons after nerve injury. J Neurosci 18:3059-3072.

Bennett DL, Boucher TJ, Armanini MP, Poulsen KT, Michael GJ, Priestley JV, Phillips HS, McMahon SB, Shelton DL. 2000 The Glial Cell Line-Derived Neurotrophic Factor Family Receptor Components Are Differentially Regulated within Sensory Neurons after Nerve Injury. The Journal of Neuroscience, 2000, 20(1):427–437.

Bisby MA, Tetzlaff W, Brown MC (1996) GAP-43 mRNA in mouse motoneurons undergoing axonal sprouting in response to muscle paralysis of partial denervation. Eur J Neurosci 8:1240-1248.

Blits, B., Oudega, M., Boer, G.J., Bartlett Bunge, M., Verhaagen, J., 2003. Adeno-associated viral vector-mediated neurotrophin gene transfer in the injured adult rat spinal cord improves hind-limb function. Neuroscience 118, 271-281.

Braz JM, Basbaum AI (2009) Triggering genetically-expressed transneuronal tracers by peripheral axotomy reveals convergent and segregated sensory neuron-spinal cord connectivity. Neuroscience 163:1220-1232.

Brenan A (1986) Collateral reinnervation of skin by C-fibres following nerve injury in the rat. Brain Res 385:152-155.

Brown MC, Holland RL, Hopkins WG (1981) Motor nerve sprouting. Annu Rev Neurosci 4:17-42.

Cafferty WB, Gardiner NJ, Das P, Qiu J, McMahon SB, Thompson SW (2004) Conditioning injury-induced spinal axon regeneration fails in interleukin-6 knock-out mice. J Neurosci 24:4432-4443.

Cafferty WB, Gardiner NJ, Gavazzi I, Powell J, McMahon SB, Heath JK, Munson J, Cohen J, Thompson SW (2001) Leukemia inhibitory factor determines the growth status of injured adult sensory neurons. J Neurosci 21:7161-7170.

Cho HJ, Kim JK, Park HC, Kim JK, Kim DS, Ha SO, Hong HS (1998) Changes in brain-derived neurotrophic factor immunoreactivity in rat dorsal root ganglia, spinal cord, and gracile nuclei following cut or crush injuries. Exp Neurol 154:224-230.

Cotman CW, Nieto-Sampedro M, Harris EW (1981) Synapse replacement in the nervous system of adult vertebrates. Physiol Rev 61:684-784.

Dahl D, Bignami A, Bich NT, Chi NH (1981) Immunohistochemical localization of the 150K neurofilament protein in the rat and the rabbit. J Comp Neurol 195:659-666.

Davis BM, Goodness TP, Soria A, Albers KM (1998) Over-expression of NGF in skin causes formation of novel sympathetic projections to trkA-positive sensory neurons. Neuroreport 9:1103-1107.

Devor M, Schonfeld D, Seltzer Z, Wall PD (1979) Two modes of cutaneous reinnervation following peripheral nerve injury. J Comp Neurol 185:211-220.

Diamond J, Cooper E, Turner C, Macintyre L (1976) Trophic regulation of nerve sprouting. Science 193:371-377.

Diamond J, Coughlin M, Macintyre L, Holmes M, Visheau B (1987) Evidence that endogenous beta nerve growth factor is responsible for the collateral sprouting, but not the regeneration, of nociceptive axons in adult rats. Proc Natl Acad Sci U S A 84:6596-6600.

Diamond J, Foerster A, Holmes M, Coughlin M (1992a) Sensory nerves in adult rats regenerate and restore sensory function to the skin independently of endogenous NGF. J Neurosci 12:1467-1476.

Diamond J, Holmes M, Coughlin M (1992b) Endogenous NGF and nerve impulses regulate the collateral sprouting of sensory axons in the skin of the adult rat. J Neurosci 12:1454-1466.

Doubleday B, Robinson PP (1994) Nerve growth factor depletion reduces collateral sprouting of cutaneous mechanoreceptive and tooth-pulp axons in ferrets. J Physiol 481 (Pt 3):709-718.

Doucette R, Diamond J (1987) Normal and precocious sprouting of heat nociceptors in the skin of adult rats. J Comp Neurol 261:592-603.

Ernfors P, Rosario CM, Merlio JP, Grant G, Aldskogius H, Persson H (1993) Expression of mRNAs for neurotrophin receptors in the dorsal root ganglion and spinal cord during development and following peripheral or central axotomy. Brain Res Mol Brain Res 17:217-226.

Fitzgerald M (1985) The sprouting of saphenous nerve terminals in the spinal cord following early postnatal sciatic nerve section in the rat. J Comp Neurol 240:407-413.

Flight RM, Harrison BJ, Mohammad F, Bunge MB, Moon, LDF, Petruska JC, Rouchka EC (2014) categoryCompare, an analytical tool based on feature annotations. Front. Genet. 5:98.

Gallo G, Lefcort FB, Letourneau PC (1997) The trkA receptor mediates growth cone turning toward a localized source of nerve growth factor. J Neurosci 17:5445-5454.

Gambetti P, Autilio GL, Papasozomenos SC (1981) Bodians silver method stains neurofilament polypeptides. Science 213:1521-1522.

Gavazzi I, Kumar RD, McMahon SB, Cohen J (1999) Growth responses of different subpopulations of adult sensory neurons to neurotrophic factors in vitro. Eur J Neurosci 11:3405-3414.

Genc B, Ulupinar E, Erzurumlu RS (2005) Differential Trk expression in explant and dissociated trigeminal ganglion cell cultures. J Neurobiol 64:145-156.

Giehl KM, Tetzlaff W (1996) BDNF and NT-3, but not NGF, prevent axotomy-induced death of rat corticospinal neurons in vivo. Eur J Neurosci 8:1167-1175.

Gloster A, Diamond J (1992) Sympathetic nerves in adult rats regenerate normally and restore pilomotor function during an anti-NGF treatment that prevents their collateral sprouting. J Comp Neurol 326:363-374.

Gloster A, Diamond J (1995) NGF-dependent and NGF-independent recovery of sympathetic function after chemical sympathectomy with 6-hydroxydopamine. J Comp Neurol 359:586-594.

Goodman LJ, Valverde J, Lim F, Geschwind MD, Federoff HJ, Geller AI, Hefti F (1996) Regulated release and polarized localization of brain-derived neurotrophic factor in hippocampal neurons. Mol Cell Neurosci 7:222-238.

Gutmann, E, 1942. Factors Affecting Recovery of Motor Function after Nerve Lesions. J Neurol Psychiatry 5, 81-95.

Harrison BJ, Venkat G, Hutson TH, Rau KK, Bunge MB, Mendell LM, Gage FH, Johnson RD, Hill CE, Rouchka EC, Moon LDF., Petruska JC, 2015. Transcriptional changes in sensory ganglion associated with primary afferent axon collateral sprouting in spared dermatome model. Genomics Data 6, 249-252.

Harrison BJ, Venkat G, Lamb J, Hutson TH, Drury C, Hill CE, Rouchka EC, Moon LDF, Petruska JC, 2016. The adapter protein CD2AP is a coordinator of neurotrophin signalling-mediated axon arbour plasticity. J Neurosci 36, 4259-4275.

Haubensak W, Narz F, Heumann R, Lessmann V (1998) BDNF-GFP containing secretory granules are localized in the vicinity of synaptic junctions of cultured cortical neurons. J Cell Sci 111 (Pt 11):1483-1493.

Healy C, LeQuesne PM, Lynn B (1996) Collateral sprouting of cutaneous nerves in man. Brain 119 (Pt 6):2063-2072.

Hill, CE, Harrison, BJ, Rau, KK, Hougland, MT, Bunge, MB, Mendell, LM, Petruska, JC, 2010. Skin incision induces expression of axonal regeneration-related genes in adult rat spinal sensory neurons. J Pain 11, 1066-1073.

Horch K (1981) Absence of functional collateral sprouting of mechanoreceptor axons into denervated areas of mammalian skin. Exp Neurol 74:313-317.

Hu-Tsai M, Winter J, Emson PC, Woolf CJ (1994) Neurite outgrowth and GAP-43 mRNA expression in cultured adult rat dorsal root ganglion neurons: effects of NGF or prior peripheral axotomy. J Neurosci Res 39:634-645.

Inbal R, Rousso M, Ashur H, Wall PD, Devor M (1987) Collateral sprouting in skin and sensory recovery after nerve injury in man. Pain 28:141-154.

Isaacson LG, Crutcher KA (1998) Uninjured aged sympathetic neurons sprout in response to exogenous NGF in vivo. Neurobiol Aging 19:333-339.

Jackson PC, Diamond J (1981) Regenerating axons reclaim sensory targets from collateral nerve sprouts. Science 214:926-928.

Jackson PC, Diamond J (1983) Failure of intact cutaneous mechanosensory axons to sprout functional collaterals in skin of adult rabbits. Brain Res 273:277-283.

Jackson PC, Diamond J (1984) Temporal and spatial constraints on the collateral sprouting of low-threshold mechanosensory nerves in the skin of rats. J Comp Neurol 226:336-345.

Jenq CB, Jenq LL, Bear HM, Coggeshall RE (1988) Conditioning lesions of peripheral nerves change regenerated axon numbers. Brain Res 457:63-69.

Kalil RE, Schneider GE (1975) Abnormal synaptic connections of the optic tract in the thalamus after midbrain lesions in newborn hamsters. Brain Res 100:690-698.

Kalous A, Keast JR (2010) Conditioning lesions enhance growth state only in sensory neurons lacking calcitonin gene-related peptide and isolectin B4-binding. Neuroscience 166:107-121.

Ketschek A, Gallo G (2010) Nerve growth factor induces axonal filopodia through localized microdomains of phosphoinositide 3-kinase activity that drive the formation of cytoskeletal precursors to filopodia. J Neurosci 30:12185-12197.

Kinnman E (1987) Collateral sprouting of sensory axons in the hairy skin of the trunk: a morphological study in adult rats. Brain Res 414:385-389.

Kobayashi NR, Fan DP, Giehl KM, Bedard AM, Wiegand SJ, Tetzlaff W (1997) BDNF and NT-4/5 prevent atrophy of rat rubrospinal neurons after cervical axotomy, stimulate GAP-43 and Talpha1-tubulin mRNA expression, and promote axonal regeneration. J Neurosci 17:9583-9595.

Koltzenburg M, Wall PD, McMahon SB (1999) Does the right side know what the left is doing? Trends Neurosci 22:122-127.

Krimm RF, Davis BM, Albers KM (2000) Cutaneous overexpression of neurotrophin-3 (NT3) selectively restores sensory innervation in NT3 gene knockout mice. J Neurobiol. 43:40-49.

Lawson SN, Waddell PJ (1991) Soma neurofilament immunoreactivity is related to cell size and fibre conduction velocity in rat primary sensory neurons. J Physiol 435:41-63.

Lorenzana AO, Lee JK, Mui M, Chang A, Zheng B (2015) A Surviving Intact Branch Stabilizes Remaining Axon Architecture after Injury as Revealed by In Vivo Imaging in the Mouse Spinal Cord. Neuron 86, 947–954.

Lu P, Jones LL, Tuszynski MH (2005) BDNF-expressing marrow stromal cells support extensive axonal growth at sites of spinal cord injury. Exp Neurol 191:344-360.

Mannion RJ, Doubell TP, Gill H, Woolf CJ (1998) Deafferentation is insufficient to induce sprouting of A-fibre central terminals in the rat dorsal horn. J Comp Neurol 393:135-144.

Mahar, M., Cavalli, V., 2018. Intrinsic mechanisms of neuronal axon regeneration. Nat Rev Neurosci 19, 323-337.

McCarter GC, Levine JD (2006) Ionic basis of a mechanotransduction current in adult rat dorsal root ganglion neurons. Mol Pain 2:28.

McCarthy PW, Lawson SN (1997) Differing action potential shapes in rat dorsal root ganglion neurones related to their substance P and calcitonin gene-related peptide immunoreactivity. J Comp Neurol 388:541-549.

McLachlan EM, Janig W, Devor M, Michaelis M (1993) Peripheral nerve injury triggers noradrenergic sprouting within dorsal root ganglia. Nature 363:543-546.

McMahon SB, Armanini MP, Ling LH, Phillips HS (1994) Expression and coexpression of Trk receptors in subpopulations of adult primary sensory neurons projecting to identified peripheral targets. Neuron 12:1161-1171.

McMahon SB, Kett-White R (1991) Sprouting of peripherally regenerating primary sensory neurones in the adult central nervous system. J Comp Neurol 304:307-315.

McQuarrie IG (1985) Effect of conditioning lesion on axonal sprout formation at nodes of Ranvier. J Comp Neurol 231:239-249.

McQuarrie IG, Grafstein B, Gershon MD (1977) Axonal regeneration in the rat sciatic nerve: effect of a conditioning lesion and of dbcAMP. Brain Res 132:443-453.

Mearow KM, Kril Y, Diamond J (1993) Increased NGF mRNA expression in denervated rat skin. Neuroreport 4:351-354.

Michael GJ, Averill S, Nitkunan A, Rattray M, Bennett DL, Yan Q, Priestley JV (1997) Nerve growth factor treatment increases brain-derived neurotrophic factor selectively in TrkA-expressing dorsal root ganglion cells and in their central terminations within the spinal cord. J Neurosci 17:8476-8490.

Michael GJ, Averill S, Shortland PJ, Yan Q, Priestley JV (1999) Axotomy results in major changes in BDNF expression by dorsal root ganglion cells: BDNF expression in large trkB and trkC cells, in pericellular baskets, and in projections to deep dorsal horn and dorsal column nuclei. Eur J Neurosci 11:3539-3551.

Nixon BJ, Doucette R, Jackson PC, Diamond J (1984) Impulse activity evokes precocious sprouting of nociceptive nerves into denervated skin. Somatosens Res 2:97-126.

Patapoutian A, Reichardt LF (2001) Trk receptors: mediators of neurotrophin action. Curr Opin Neurobiol 11:272-280.

Pertens E, Urschel-Gysbers BA, Holmes M, Pal R, Foerster A, Kril Y, Diamond J (1999) Intraspinal and behavioral consequences of nerve growth factor-induced nociceptive sprouting and nerve growth factor-induced hyperalgesia compared in adult rats. J Comp Neurol 410:73-89.

Petruska, J.C., Barker, D.F., Garraway, S.M., Trainer, R., Fransen, J.W., Seidman, P.A., Soto, R.G., Mendell, L.M., Johnson, R.D., 2014. Organization of sensory input to the nociceptive-specific cutaneous trunk muscle reflex in rat, an effective experimental system for examining nociception and plasticity. J Comp Neurol 522, 1048-1071.

Phillips LL, Autilio-Gambetti L, Lasek RJ (1983) Bodians silver method reveals molecular variation in the evolution of neurofilament proteins. Brain Res 278:219-223.

Ramon y Cajal S (1928) Degeneration and regeneration of the Nervous System. London: Oxford University Press.

Richardson PM, Verge VM (1987) Axonal regeneration in dorsal spinal roots is accelerated by peripheral axonal transection. Brain Res 411:406-408.

Robinson PP (1988) Observations on the recovery of sensation following inferior alveolar nerve injuries. Br J Oral Maxillofac Surg 26:177-189.

Rosenzweig, E.S., Courtine, G., Jindrich, D.L., Brock, J.H., Ferguson, A.R., Strand, S.C., Nout, Y.S., Roy, R.R., Miller, D.M., Beattie, M.S., Havton, L.A., Bresnahan, J.C., Edgerton, V.R., Tuszynski, M.H., 2010. Extensive spontaneous plasticity of corticospinal projections after primate spinal cord injury. Nat Neurosci 13, 1505-1510.

Ruscheweyh R, Forsthuber L, Schoffnegger D, Sandkuhler J (2007) Modification of classical neurochemical markers in identified primary afferent neurons with Abeta-, Adelta-, and C-fibers after chronic constriction injury in mice. J Comp Neurol 502:325-336.

Schneider GE (1973) Early lesions of superior colliculus: factors affecting the formation of abnormal retinal projections. Brain Behav Evol 8:73-109.

Shi TJ, Tandrup T, Bergman E, Xu ZQ, Ulfhake B, Hokfelt T (2001) Effect of peripheral nerve injury on dorsal root ganglion neurons in the C57 BL/6J mouse: marked changes both in cell numbers and neuropeptide expression. Neuroscience 105:249-263.

Skene JH (1984) Growth-associated proteins and the curious dichotomies of nerve regeneration. Cell 37:697-700.

Smith DS, Skene JH (1997) A transcription-dependent switch controls competence of adult neurons for distinct modes of axon growth. J Neurosci 17:646-658.

Snider WD, Zhou FQ, Zhong J, Markus A (2002) Signaling the pathway to regeneration. Neuron 35:13-16.

Theriault E, Diamond J (1988) Nociceptive cutaneous stimuli evoke localized contractions in a skeletal muscle. J Neurophysiol 60:446-462.

Tobias CA, Shumsky JS, Shibata M, Tuszynski MH, Fischer I, Tessler A, Murray M (2003) Delayed grafting of BDNF and NT-3 producing fibroblasts into the injured spinal cord stimulates sprouting, partially rescues axotomized red nucleus neurons from loss and atrophy, and provides limited regeneration. Exp Neurol 184:97-113.

Tsujino, H., Kondo, E., Fukuoka, T., Dai, Y., Tokunaga, A., Miki, K., Yonenobu, K., Ochi, T., Noguchi, K., 2000. Activating transcription factor 3 (ATF3) induction by axotomy in sensory and motoneurons: A novel neuronal marker of nerve injury. Mol Cell Neurosci 15, 170-182.

Tucker BA, Rahimtula M, Mearow KM (2005) A procedure for selecting and culturing subpopulations of neurons from rat dorsal root ganglia using magnetic beads. Brain Res Brain Res Protoc 16:50-57.

Vavrek R, Girgis J, Tetzlaff W, Hiebert GW, Fouad K (2006) BDNF promotes connections of corticospinal neurons onto spared descending interneurons in spinal cord injured rats. Brain 129:1534-1545.

Woolf CJ, Shortland P, Sivilotti LG (1994) Sensitization of high mechanothreshold superficial dorsal horn and flexor motor neurones following chemosensitive primary afferent activation. Pain 58:141-155.

Ygge J (1984) On the organization of the thoracic spinal ganglion and nerve in the rat. Exp Brain Res 55:395-401.

ZGraggen WJ, Fouad K, Raineteau O, Metz GA, Schwab ME, Kartje GL (2000) Compensatory sprouting and impulse rerouting after unilateral pyramidal tract lesion in neonatal rats. J Neurosci 20:6561-6569.

Figure Legends

Figure 1 Schematic showing the central and peripheral branches of thoracic DRG neurons before and after induction of PACS. (A) Thoracic DRG neurons (orange) exhibit a 1:1:1 correspondence between a spinal cord segment (blue), DRG and the dermatome they innervate (yellow). **(B)** Transection and ligation of cutaneous nerves (red crosses) neighbouring the spared T11 nerve (orange) leaves a cutaneous sensory field innervated by the uninjured DRG neurons and surrounded by a vast area of denervation. **(C)** Over time, the peripheral branch of the spared, uninjured "T11 PACS DRG" (green) undergoes primary afferent collateral sprouting to innervate previously denervated areas to restore sensorimotor reflexes and function. In this study the "contralateral T11 DRG" was used as a control. The "contralateral-to-transection DRGs" (T9, T10, T12, T13) were pooled and also used as controls.

Figure 2. The response to pinching is lost in a denervated zone created by transection of cutaneous nerves but is restored after collateral sprouting by uninjured neurons from the spared T11 DRG. (A) The CTM reflex response in the thoracolumbar region activates a functionally appropriate segmental muscle. **(B)** Pinch evokes contraction of the skin in normal, lightly anesthetised rats. Images in A and B are from Theriault and Diamond (1988). **(C)** Following cutaneous nerve transection, behavioural "pinch mapping" reveals areas exhibiting a presence or absence of the CTM reflex response (denoted by black lines and arrows). The blue line indicates the responsive "isolated" mechanonociceptive field and red lines denote unresponsive mechanonociceptive fields. **(D)** At 14 days after surgery, "pinch

mapping" in the same rat showed expansion of the zone exhibiting a CTM reflex response (denoted by white arrows and blue line); previous borders are denoted by black arrows. Regions of denervation had shrunk (denoted by red lines). **(C-D)** Scale bars: 0.5 mm.

Figure 3: The neuronal injury marker ATF3 was not expressed in DRG neurons undergoing PACS. Whereas (A) very few neurons showed immunoreactivity for ATF3 in naïve DRG. (B) ATF3 was expressed in large numbers of neurons from from a positive control tissue (a lumbar DRG whose peripheral branch was transected seven days previously). In contrast, very few neurons showed immunoreactivity for ATF3 in DRG taken either (C) 7 days or (D) 14 days after induction of PACS. Nuclei were counterstained using bisbenzamide (blue). Scale bar, 50 µm.

Figure 4: DRG neurons from naïve rats extended neurites poorly in the first 18 hours *in vitro* but arborized by 24 hours. Photomicrographs of dissociated adult DRG neurons from naive animals after **(A, B)** 18 hr and **(C, D)** 24 hr after initial plating *in vitro*. Cultures were fixed and immunostained for βIII tubulin to visualise neurites (red) and CGRP (green). Observations revealed less neurite outgrowth after 18 hr where neurons exhibited **(A, B)** short arborizing neurites compared to the **(C, D)** long arborizing neurites found after 24 hr of plating. Scale bars: **(A, C)** 300 µm, **(B)** 20 µm, **(D)** 100 µm.

Figure 5: Uninjured neurons from T11 DRGs that had undergone PACS exhibited axonal elongation more frequently than naive contralateral T11 neurons *in vitro*. Photomicrographs show adult DRG neurons after 18 hr in culture. They were explanted and dissociated **(A-D)** 7 days and **(E-I)** 14 days after induction of PACS. **(B,G)** Transected neurons were found to extend sparsely branched, elongating neurites at both 7 and 14 days after surgery. **(A,E,F)** Uninjured T11 neurons that were dissociated 14 days after induction of PACS extended long neurites, similar to transected neurons. Scale bar: 200 µm

Figure 6: Uninjured neurons from T11 DRGs that had undergone PACS arborized more frequently than naive contralateral T11 DRG neurons. Photomicrographs of dissociated adult DRG neurons ipsilateral and contralateral to transection observed exhibiting an arborizing pattern growth after **(A-D)** 7 days and **(E-H)** 14 days after 18 hr *in vitro*. Some uninjured and transected neurons were found to extend more highly branched, longer neurites at **(E-F)** 14 days compared to **(A-B)** 7 days after surgery.

Figure 7: Uninjured neurons that had undergone PACS extend longer neurites *in vitro* than uninjured neurons that had not undergone PACS. (A', A'') Neurons with processes

greater than 10 µm were counted. (**B)** The percentage of neurons initiating outgrowth greater than 10 µm was higher from uninjured PACS DRGs and from transected DRGs compared to naïve DRGs (p <0.05). **(C', C'')** Neurons with processes over 50 µm were included in a Sholl analysis. Scale bar: 50 µm. **(D)** The percentage of neurons with neurites over 50 µm was higher from uninjured T11 PACS DRGs and from transected DRGs compared to naïve DRGs. **(E)** Analysis of mean neurite length showed that the sprouting neurons from uninjured (PACS) and transected DRGs sprouted longer neurites compared to naive. Results are presented as mean ± SEM and were analysed using Mann Whitney (groups compared to naive neurons) and Wilcoxon (groups compared to contralateral control neurons). Significance is denoted as: * $p < 0.05$, ** $p < 0.01$, *** $p < 0.001$ (7 days, $n = 4$; 14 days, $n = 3$).

Figure 8: (A) A larger percentage of neurons from PACS DRGs and Transected DRGs elongated relative to those from naïve DRGs both 7 and 14 days after induction of PACS. Transected neurons also displayed an enhanced regenerative response at 14 days compared to 7 days after induction of PACS. **(B)** A larger percentage of neurons from PACS DRGs and Transected DRGs arborized relative to those from naïve DRGs only 14 days after induction of PACS. The percentage was larger at 14 days than at 7 days for both PACS DRGs and Transected DRGs. Results were analysed using Mann Whitney (groups compared to naive neurons) and Wilcoxon (groups compared to contralateral control neurons). Significance is denoted as: * $p < 0.05$, ** $p < 0.01$, *** $p < 0.001$. All results are presented as mean ± SEM.

Figure 9: Sprouting PACS neurons show a higher incidence of an elongating or arborizing phenotype than naïve neurons. Sholl analysis was used to quantify total neurite lengths and number of branches at each shell distance from DRG neurons dissociated **(A, C)** 7 days and **(B, D)** 14 days after induction of PACS. Results were analysed using two-way RM ANOVA with LSD *post hoc* tests. Mean ± SEM. Significance is denoted as: Spared T11 vs Naive, X $p < 0.05$, XXX $p < 0.001$; Transected vs Naive, * $p < 0.05$, ** $p < 0.01$, *** $p < 0.001$; Transected vs. Contralateral-to-transected DRGs, + $p < 0.05$, +++ $p < 0.001$. Bracket on the right-hand side denotes significance of pairwise group effect; symbols above error bars denotes significant *post hoc* test result.

Figure 10: The majority of sprouting neurons had small diameters. Histograms show the cell diameter distribution for all **(A)** sprouting, **(C)** elongating and **(E)** arborizing neurons in the uninjured T11 DRG. **(B, D, F)** Cells were categorised as small diameter (<35 µm) or large diameter (>35 µm) sprouting neurons. **(B)** The majority of sprouting neurons were found to be small diameter neurons, including **(D)** elongating and **(F)** arborizing types. Results are presented as mean ± SEM and were analysed using the Wilcoxon test (related measures) or Mann Whitney test (7d v 14d). Significance is denoted as: * $p < 0.05$.

Figure 11: Sprouting neurons are mostly CGRP negative. (A) More sprouting neurons in PACS and transected DRGs were CGRP negative than positive. Results are presented as mean ± SEM and were analysed using the Wilcoxon test. Significance is denoted as: * $p < 0.05$, *** $p < 0.001$. **(B-C)** Photomicrographs of dissociated adult neurons from the uninjured T11 DRG were immunolabelled for CGRP at 14 days after induction of PACS. **(B)** CGRP positive labelling were found in small diameter sprouting neurons. Sprouting neurons that were negatively labelled for CGRP had either large or small somata. Scale bar: 50 µm

Figure 1

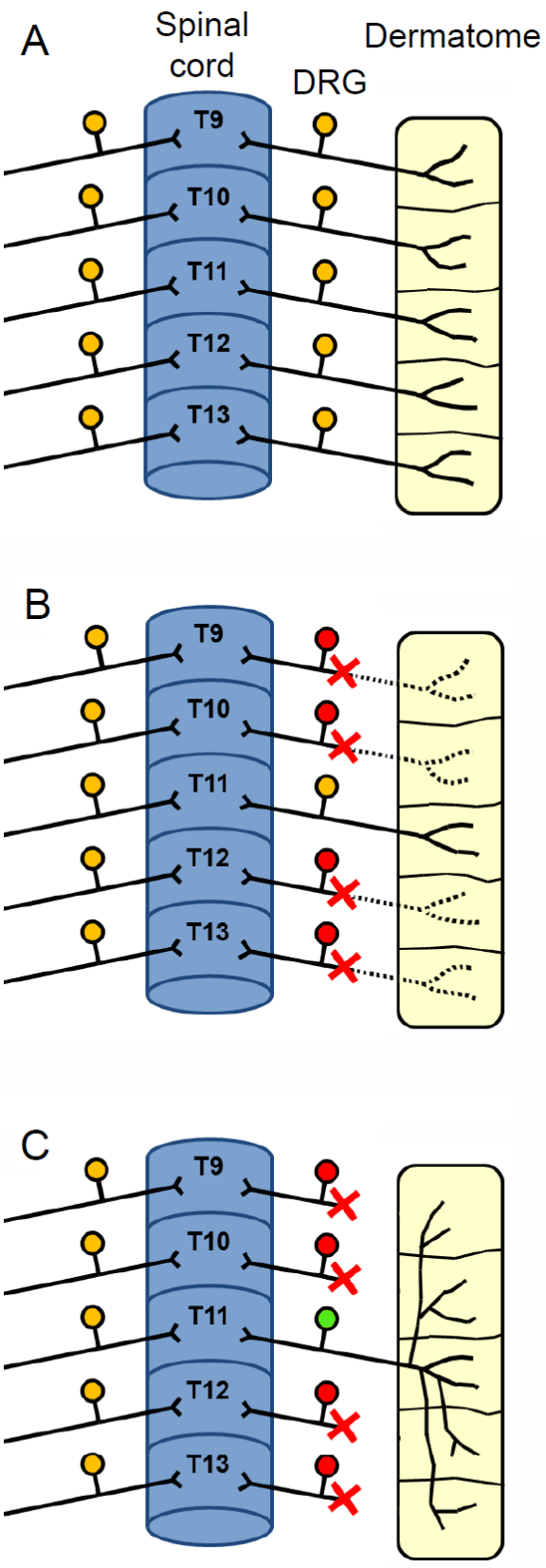
A
Spinal cord
DRG
Dermatome
T9
T10
T11
T12
T13
B
T9
T10
T11
T12
T13
C
T9
T10
T11
T12
T13

Figure 2

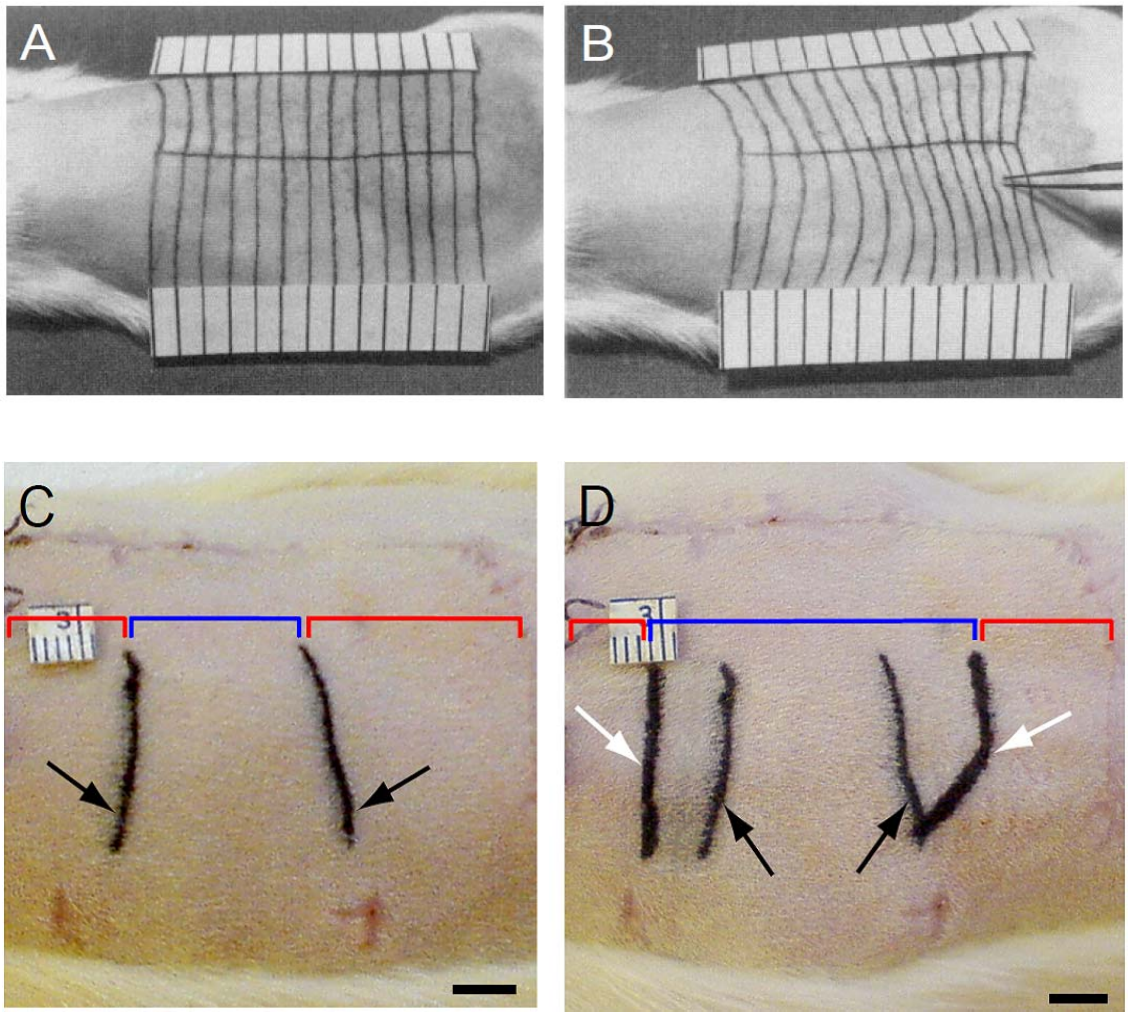

Figure 3

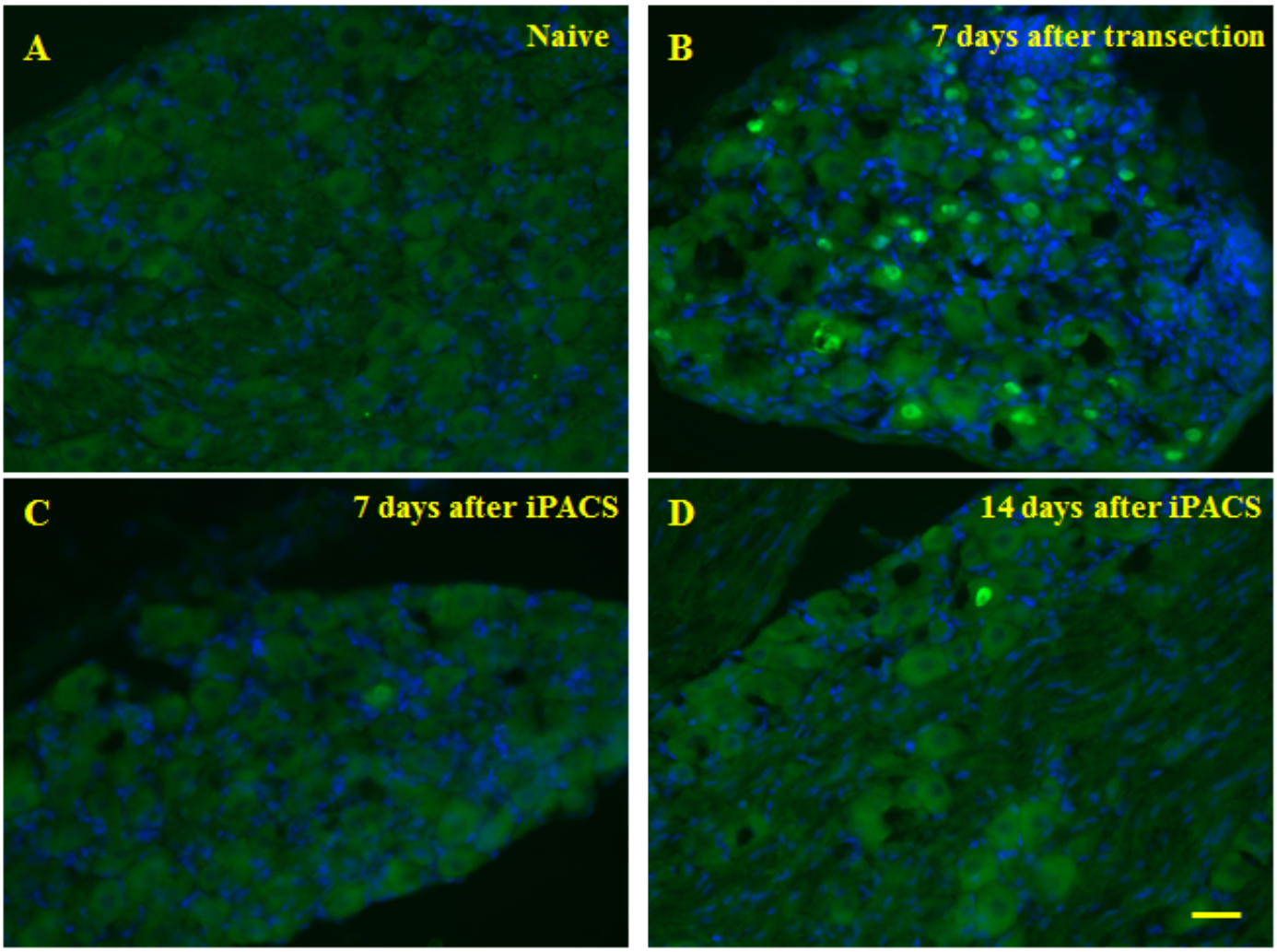
A
Naive
B
7 days after transection
C
7 days after iPACS
D
14 days after iPACS

Figure 4

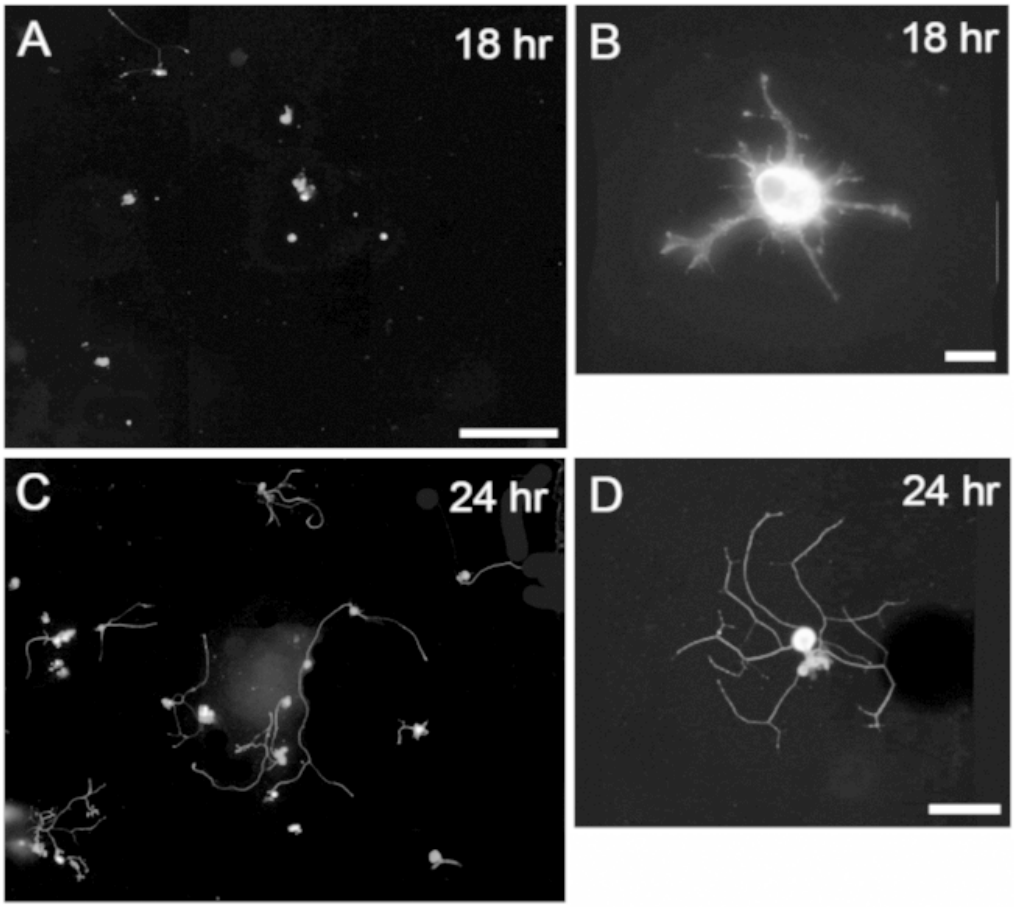

Figure 5

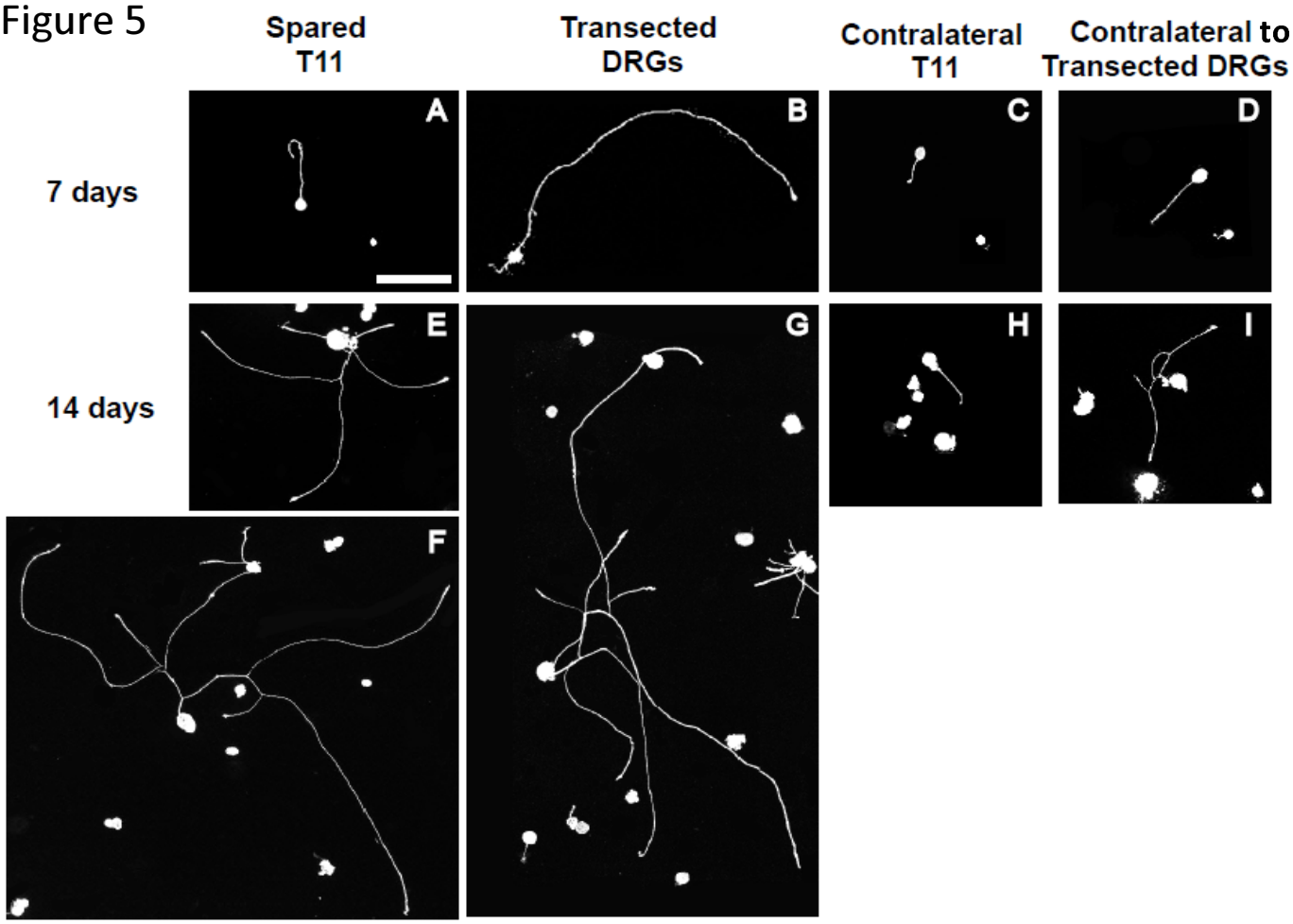
Spared T11
Transected DRGs
Contralateral T11
Contralateral to Transected DRGs
7 days
14 days
A
B
C
D
E
F
G
H
I

Figure 6

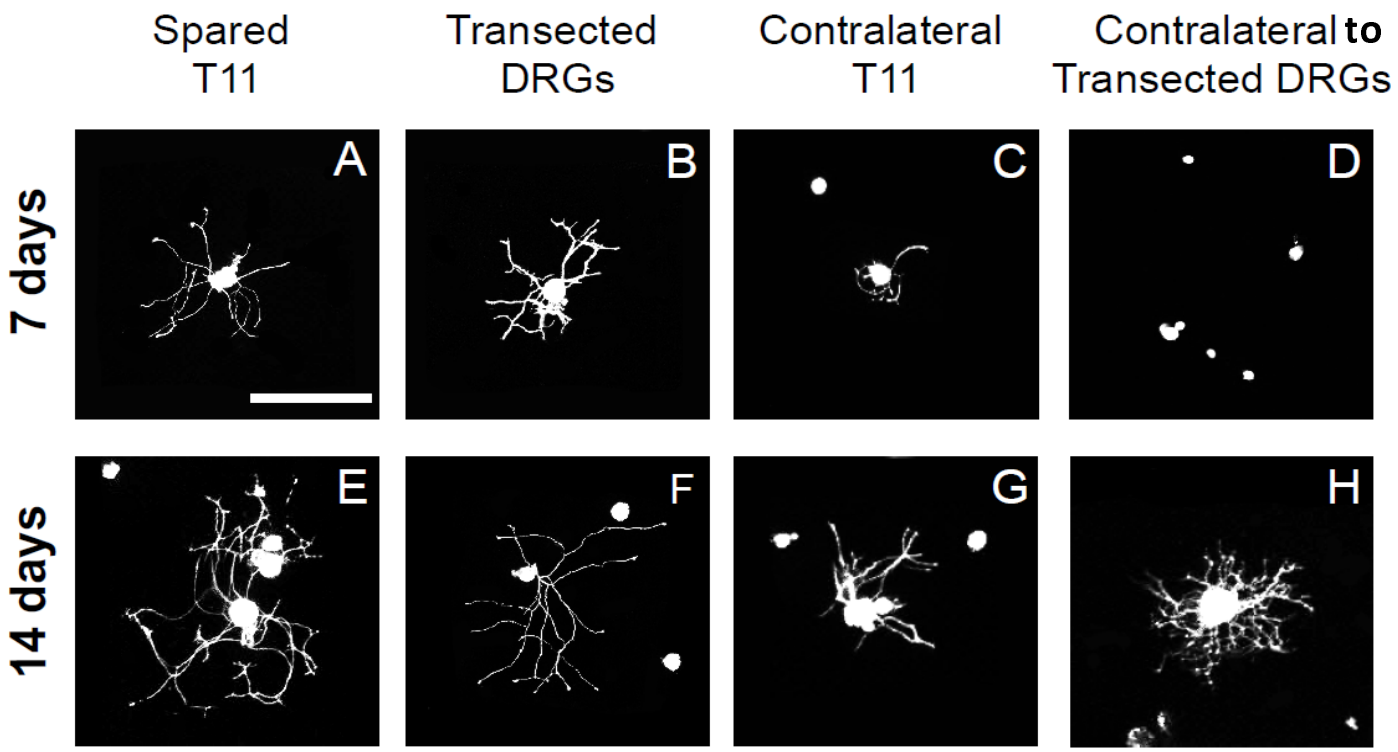
Spared T11
Transected DRGs
Contralateral T11
Contralateral to Transected DRGs
7 days
14 days
A
B
C
D
E
F
G
H

Figure 7

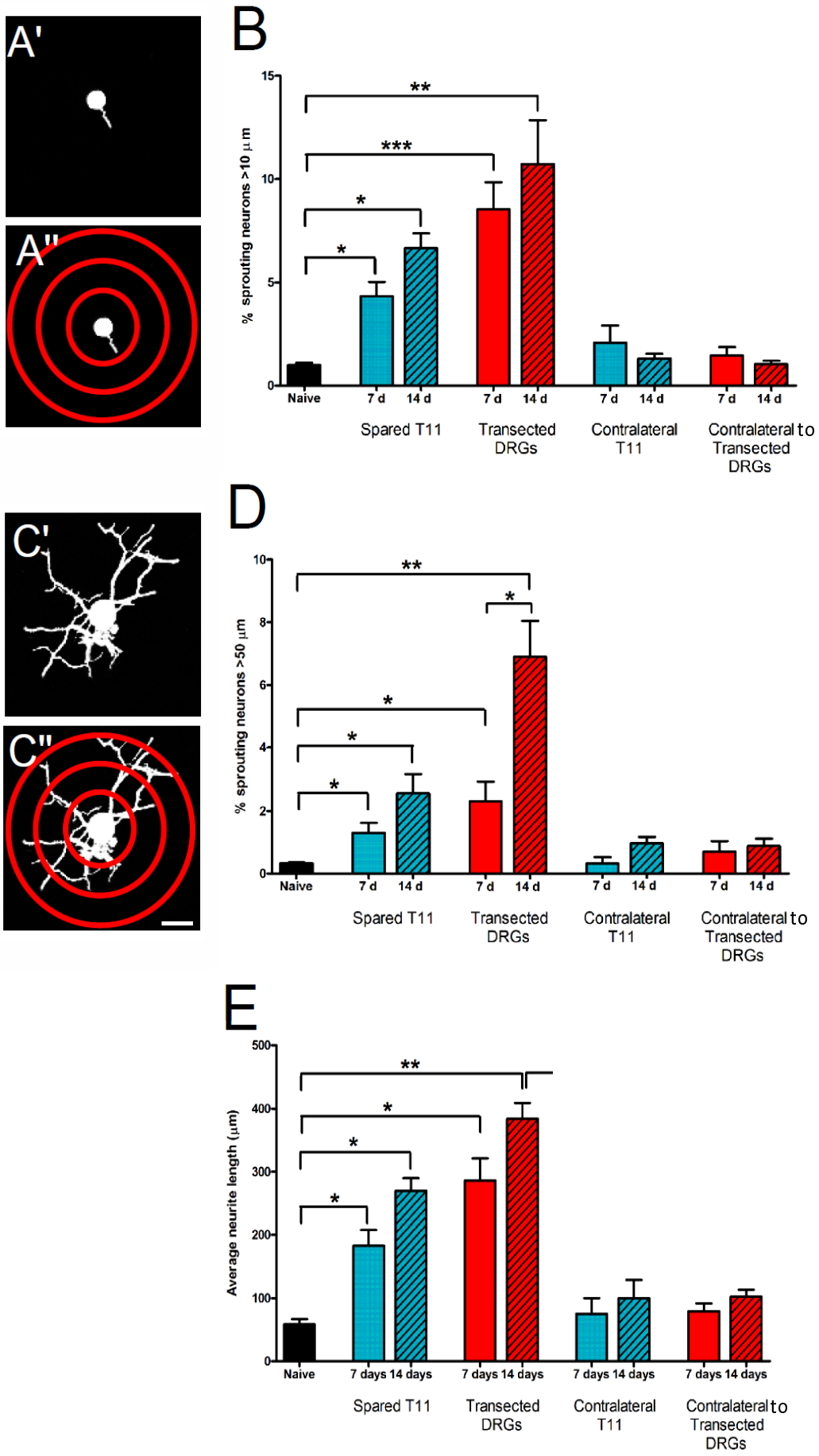
A'
A''
B
% sprouting neurons >10 µm
15
10
5
0
**
***
*
*
Naive
7 d
14 d
7 d
14 d
7 d
14 d
7 d
14 d
Spared T11
Transected DRGs
Contralateral T11
Contralateral to Transected DRGs
C'
C''
D
% sprouting neurons >50 µm
10
8
6
4
2
0
**
*
*
*
*
Naive
7 d
14 d
7 d
14 d
7 d
14 d
7 d
14 d
Spared T11
Transected DRGs
Contralateral T11
Contralateral to Transected DRGs
E
Average neurite length (µm)
500
400
300
200
100
0
**
*
*
*
Naive
7 days
14 days
7 days
14 days
7 days
14 days
7 days
14 days
Spared T11
Transected DRGs
Contralateral T11
Contralateral to Transected DRGs

Figure 8

A

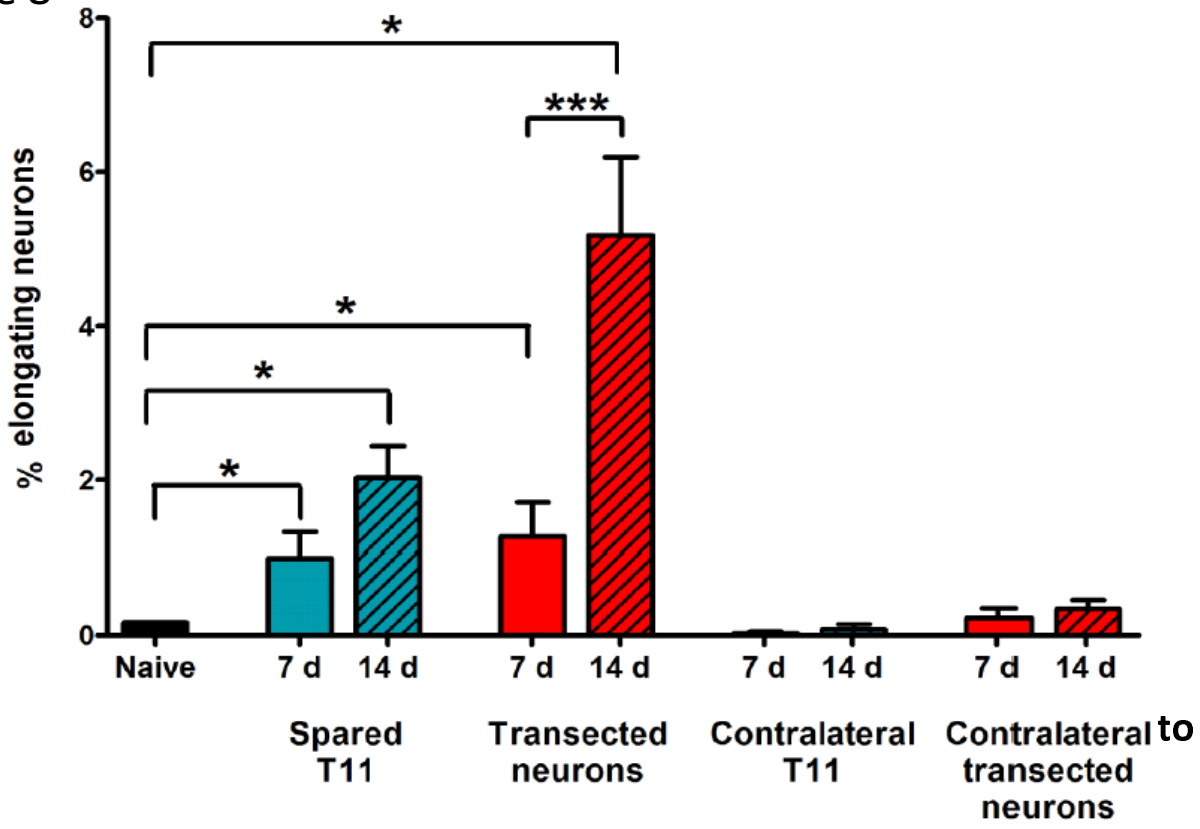
% elongating neurons
8
6
4
2
0
*
***
*
*
*
Naive
7 d
14 d
7 d
14 d
7 d
14 d
7 d
14 d
Spared T11
Transected neurons
Contralateral T11
Contralateral to transected neurons

B

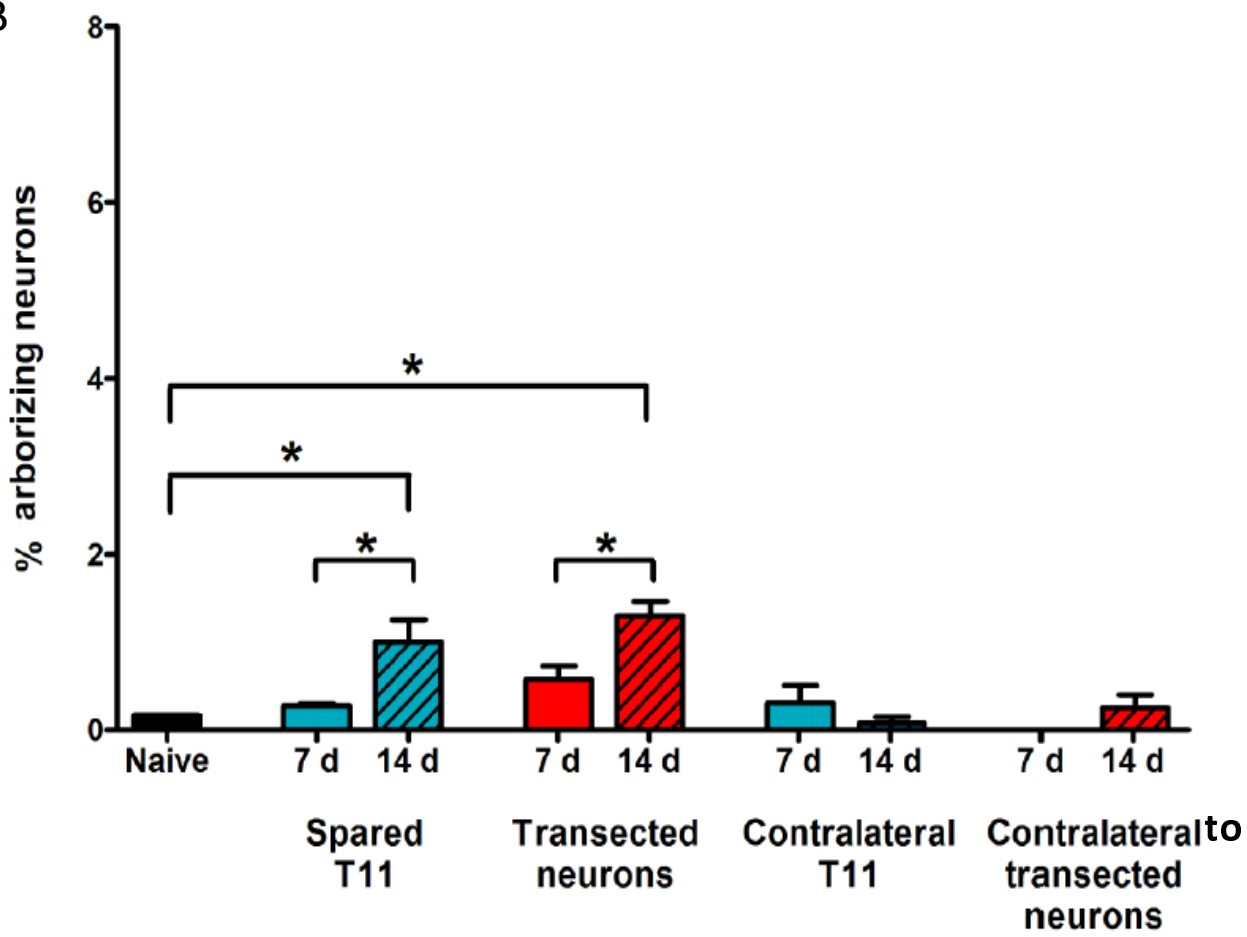
% arborizing neurons
8
6
4
2
0
*
*
*
*
Naive
7 d
14 d
7 d
14 d
7 d
14 d
7 d
14 d
Spared T11
Transected neurons
Contralateral T11
Contralateral to transected neurons

Figure 9

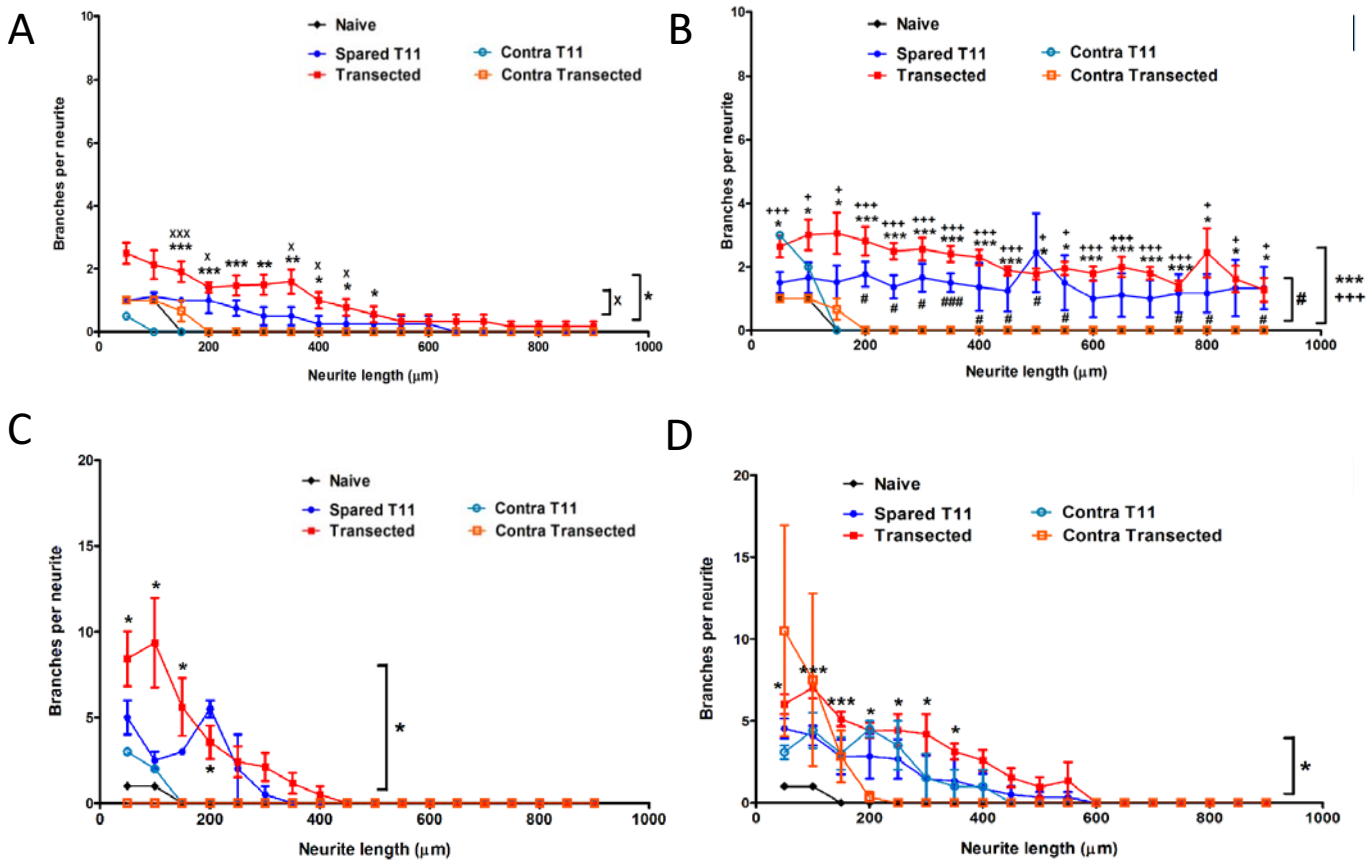
A
B
C
D
Naive
Spared T11
Transected
Contra T11
Contra Transected
Branches per neurite
Neurite length (µm)

Figure 10

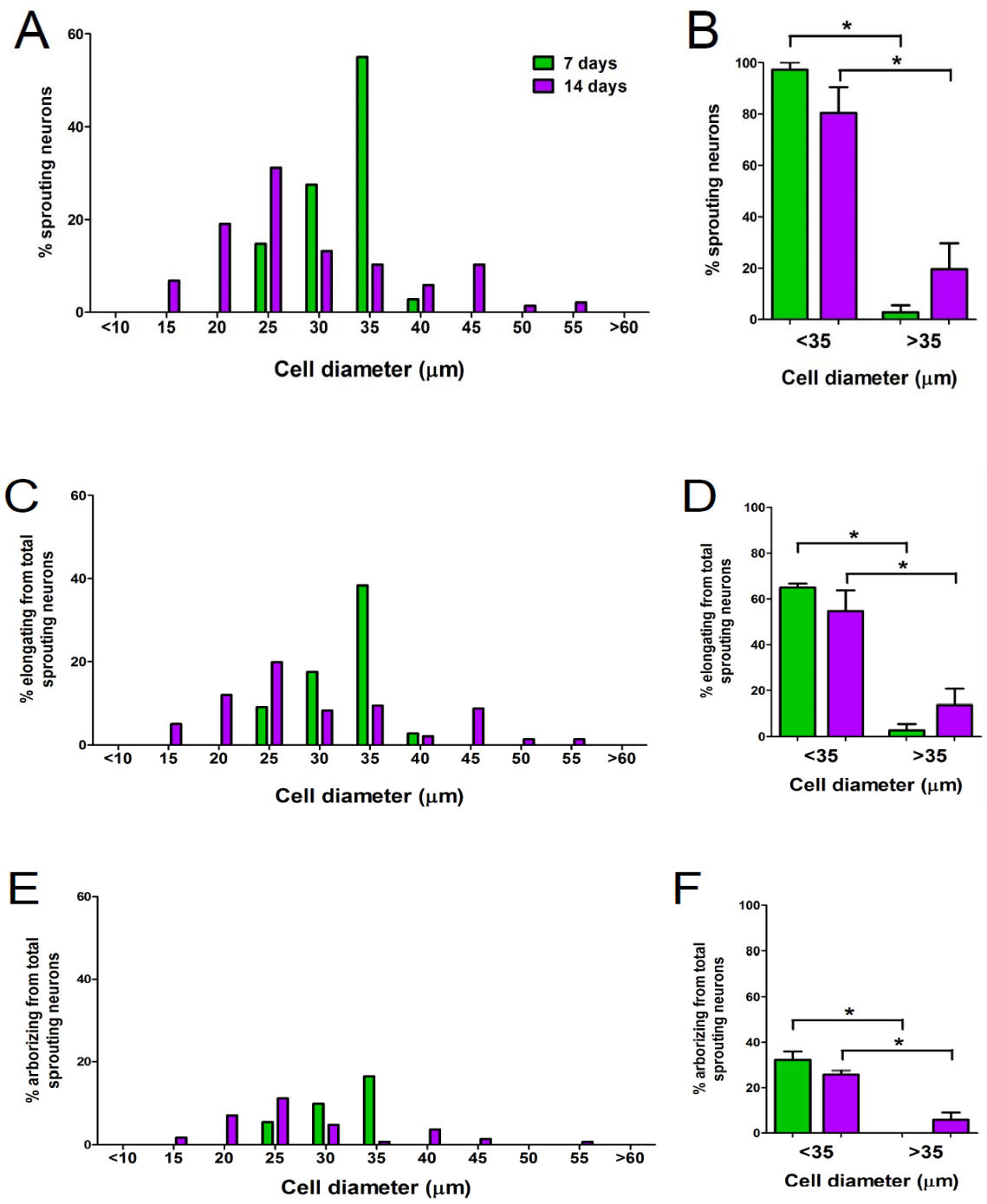
A
% sprouting neurons
7 days
14 days
<10
15
20
25
30
35
40
45
50
55
>60
Cell diameter (μm)
B
% sprouting neurons
<35
>35
Cell diameter (μm)
C
% elongating from total sprouting neurons
Cell diameter (μm)
D
% elongating from total sprouting neurons
Cell diameter (μm)
E
% arborizing from total sprouting neurons
Cell diameter (μm)
F
% arborizing from total sprouting neurons
Cell diameter (μm)

Figure 11

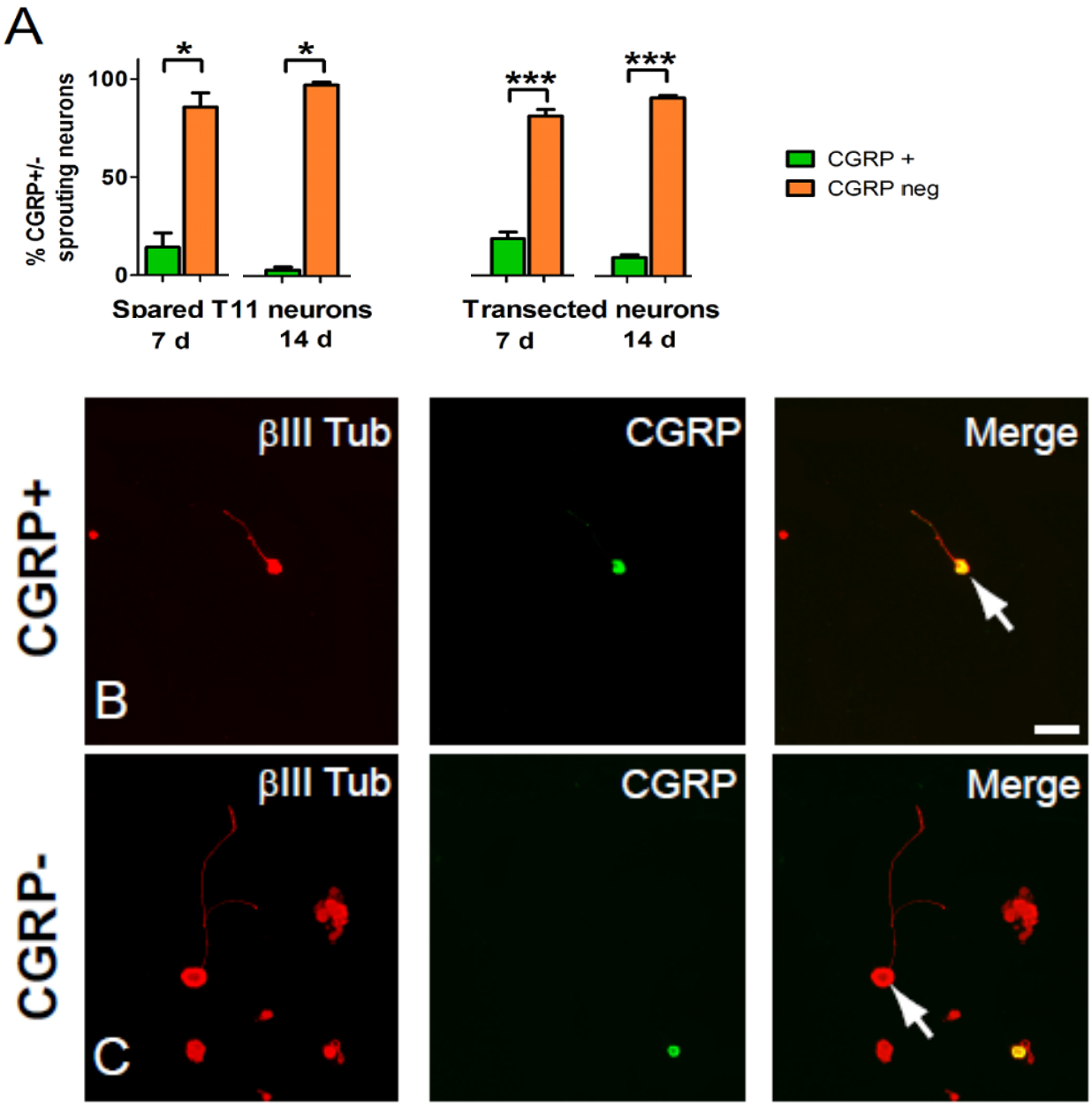
A
% CGRP+/- sprouting neurons
100
50
0
*
*
***
***
Spared T11 neurons
7 d
14 d
Transected neurons
7 d
14 d
CGRP +
CGRP neg
CGRP+
CGRP-
βIII Tub
CGRP
Merge
B
C